

**The Influence of Defects in Concrete (Cracking and Consolidation)
on Water Absorption and Electrical Conductivity**

Shahrzad Eghtesadi

A Thesis

in

The Department

of

Building, Civil, and Environmental Engineering

Presented in Partial Fulfillment of the Requirements

For the Degree of Master of Applied Science (Civil Engineering) at

Concordia University

Montréal, Québec, Canada

August 2014

© Shahrzad Eghtesadi, 2014

CONCORDIA UNIVERSITY

School of Graduate Studies

This is to certify that the thesis prepared

By: Shahrzad Eghtesadi

Entitled: The influence of concrete defects (cracking and consolidation) on water absorption and electrical conductivity

and submitted in partial fulfillment of the requirements for the degree of

Master of Applied Science (Civil Engineering)

complies with the regulations of the University and meets the accepted standards with respect to originality and quality.

Signed by the final examining committee:

<u>Dr. Lan Lin</u>	Chair
<u>Dr. Hua Ge</u>	Examiner
<u>Dr. Martin Pugh</u>	Examiner
<u>Dr. Michelle Nokken</u>	Supervisor

Approved by _____
Chair of Department or Graduate Program Director

August 2014 _____
Dean of Faculty

ABSTRACT

The influence of defects in concrete (cracking and consolidation) on water absorption and electrical conductivity

Shahrzad Eghtesadi

The great impact of durability on concrete performance and service life makes it a serious issue in the recent years. Cracking plays an important role in increasing the mass transport properties of concrete thus decreasing its durability against harsh environmental conditions. Construction defects such as improper consolidation is another factor leading to the unacceptably high rate of concrete deterioration.

In this research, several concrete specimens were manufactured with two different water-cement ratios. The influence of cracking induced by both mechanical and thermal loading on mass transport properties of concrete was studied. Further, the effect of construction practices including over-vibration and insufficient consolidation on concrete properties was investigated. Ultrasonic pulse velocity was applied to identify the presence of internal damage. Water absorption, electrical conductivity and electrical resistivity are the main standard test methods used for durability evaluation.

It was found that water absorption and electrical conductivity of concrete are not significantly affected by the formation of localized bond cracking under short term tensile loading below 80% of the ultimate capacity. However, the well distributed network of shrinkage cracking associated with rapid microwave heating can accelerate the rate of water and chloride ingress through concrete to the large extent. Results also showed that the presence of large, interconnected voids

induced by insufficient degree of consolidation has much more destructive influence on concrete microstructure.

ACKNOWLEDGEMENTS

First and foremost, I would like to express my sincere appreciation to my supervisor Dr. Michelle Nokken for all her support, guidance, inspiration and patience during my studies. Without her significant support in all aspects of my research, this thesis would not have been accomplished.

I wish to extend my especial gratitude to my beloved family for their endless love, patience and sacrifice.

Also, I sincerely thank my senior colleagues Arash Rahmatian, Sajjad Mirvalad and Javad Mirvalad for sharing their experience and insight.

In addition, I would like to thank Mr. Joseph Hrib, Mr. Jamie Yeargans and Mr. Luc Demers for training me and providing me with laboratory equipment at Concordia University's department of Building, Civil and Environmental Engineering.

Finally, I dedicate this thesis to my best friend, Babak Mohammadi, to whom I am deeply indebted for his continuous and unconditional help and encouragement throughout my work. It is impossible to find the words to fully thank him.

Table of Contents

Table of Figures	ix
Table of Tables.....	xii
1 INTRODUCTION	1
1.1 GENERAL DESCRIPTION.....	1
1.2 RESEARCH OBJECTIVES.....	4
1.3 ORGANIZATION OF THE THESIS	5
2 LITERATURE REVIEW	6
2.1 INTRODUCTION	6
2.2 CONCRETE DURABILITY	6
2.3 DIFFERENT MASS TRANSPORT MECHANISMS IN CONCRETE.....	8
2.3.1 Absorption.....	8
2.3.2 Permeability	11
2.3.3 Diffusion.....	12
2.4 DIFFERENT CAUSES OF CRACKING IN CONCRETE.....	13
2.4.1 Cracking occurred before hardening.....	14
2.4.2 Cracking occurring after hardening.....	16
2.5 FRACTURE OF PLAIN CONCRETE UNDER MECHANICAL LOADING.....	18
2.6 METHODS FOR MICROCRACK DETECTION IN CONCRETE.....	21
2.7 EFFECT OF CRACKING ON CONCRETE DETERIORATION.....	25
2.7.1 Summary	35
2.8 CONCRETE BEHAVIOR UNDETR ELEVATED TEMPERATURE	37

2.9	THE EFFECT OF CONSOLIDATION ON CONCRETE PROPERTIES	42
2.10	RESEARCH MOTIVATION	48
3	EXPERIMENTAL PROGRAM	51
3.1	GENERAL DESCRIPTION	51
3.2	MATERIALS	52
3.3	SPECIMEN DETAILS	54
3.3.1	Phases 1 and 2	54
3.3.2	Phases 3	54
3.4	TESTING PROCEDURES	57
3.4.1	Splitting tensile test	57
3.4.2	Microwave heating	59
3.4.3	Ultrasonic pulse velocity	60
3.4.4	Water absorption	62
3.4.5	Bulk electrical conductivity	64
3.4.6	Bulk electrical resistivity	67
4	RESULTS AND DISCUSSION	69
4.1	INTRODUCTION	69
4.2	RESULTS FOR PHASE 1	70
4.2.1	The effect of load-induced cracking on ultrasonic pulse velocity	70
4.2.2	The effect of load-induced cracking on water absorption	72
4.2.3	The effect of load-induced cracking on electrical conductivity	76
4.3	RESULTS FOR PHASE 2	78

4.3.1	The effect of thermal induced cracking on ultrasonic pulse velocity	78
4.3.2	The effect of thermally-induced cracking on water absorption and electrical conductivity	81
4.4	RESULTS FOR PHASE 3.....	84
4.4.1	The effect of consolidation degree on compressive strength of concrete	84
4.4.2	The effect of consolidation degree on ultrasonic pulse velocity.....	86
4.4.3	The effect of consolidation degree on the water absorption test.....	88
4.4.4	The effect of consolidation degree on bulk electrical conductivity and bulk electrical resistivity.....	91
5	CONCLUSIONS AND RECOMMENDATIONS	93
5.1	CONCLUSIONS	93
5.2	RECOMMENDATIONS.....	96
6	REFERENCES	97

Table of Figures

Figure 2.1 Schematic of the sorptivity test (ASTM C 1585-04).....	10
Figure 2.2 Typical water absorption test data (ASTM C1585-04).....	11
Figure 2.3 Different types of cracking (Heran 1999)	20
Figure 2.4 Schematic of pulse velocity apparatus (ASTM C 597-09).....	22
Figure 2.5 Decrease in UPV versus different compressive stress levels (after Raju 1997).....	24
Figure 2.6 Coefficient of permeability for stressed and unstressed specimens at 7 days (Bhargva and Banthia 2006).....	26
Figure 2.7 Normalized charge passed against compressive stress levels (Samaha and Hover 1992).....	27
Figure 2.8 Water absorption versus time for different load percentages (Samaha and Hover 1992).....	28
Figure 2.9 Charge passed against different stress levels (Saito and Ishimori 1995)	29
Figure 2.10 Coefficient of permeability versus stress levels (Hearn 1999).....	30
Figure 2.11 Water permeability versus crack opening displacement (Aldea et al. 1999)	31
Figure 2.12 Initial current versus crack opening displacement (Aldea et al. 1999)	32
Figure 2.13 Average crack area before and after loading (Lim et al. 2000).....	33
Figure 2.14 RCPT results for different stress-strength ratios (Lim et al. 2000)	33
Figure 2.15 Electrical conductivity against different stress-strength ratios (Yang et al. 2006)...	34
Figure 2.16 AE versus water absorption at 90% of tensile strength loading (Yang et al. 2006).	35
Figure 2.17 Drying shrinkage cracking (Hearn 1999).....	38
Figure 2.18 Effect of drying on total charge passed (Samaha and Hover 1992).....	39
Figure 2.19 The influence of drying treatment on water absorption (Martys and Ferraris 1997)	40

Figure 2.20 Coefficient of permeability versus time (Hearn 1999).....	41
Figure 2.21 The effect of temperature on permeability without mechanical loading (Choinska et al. 2007)	42
Figure 2.22 Different void contents versus concrete properties (Kaplan 1960).....	45
Figure 2.23 Relation between the charge passed and degree of consolidation (Whiting et al. 1987).....	46
Figure 2.24 Relation between 28-day compressive strength and degree of consolidation (Whiting et al. 1987)	46
Figure 2.25 Location effect on the UPV of concrete and paste (Popovics et al. 1990).....	47
Figure 2.26 Location effect on chloride permeability of concrete (Aldea et al. 1999).....	48
Figure 3.1 Samples in the curing bath	54
Figure 3.2 Surface appearance of unconsolidated sample (left) versus full compacted sample (right)	55
Figure 3.3 Brazilian test setup	58
Figure 3.4 Temperature measurements after microwave heating.....	59
Figure 3.5 Ultrasonic pulse velocity test device	60
Figure 3.6 Samples in an environmental chamber.....	63
Figure 3.7 Water absorption test setup	64
Figure 3.8 Vacuum saturation device	66
Figure 3.9 Bulk electrical conductivity test set up.....	66
Figure 3.10 PROCEQ unit used to measure the electrical resistivity	68
Figure 4.1 Effect of tensile loading on pulse velocity of concrete	71
Figure 4.2 Microcrack recovery after unloading (Lim et al. 2000)	72

Figure 4.3 Water absorption results for specimens at stress-free state	73
Figure 4.4 Initial water sorptivity versus stress-strength ratio.....	74
Figure 4.5 Secondary water sorptivity versus stress-strength ratio	74
Figure 4.6 Bulk electrical conductivity versus stress-strength ratio	77
Figure 4.7 Normalized electrical conductivity versus stress-strength ratio	78
Figure 4.8 Temperature versus heating time.....	79
Figure 4.9 The effect of microwave heating on concrete mass and UPV for w/c=0.4	80
Figure 4.10 The effect of microwave heating on concrete mass and UPV for w/c=0.5	80
Figure 4.11 Relationship between initial sorptivity and heating time	82
Figure 4.12 Relationship between secondary sorptivity and heating time	82
Figure 4.13 Relationship between bulk electrical conductivity and heating time	83
Figure 4.14 Relationship between normalized electrical conductivity and heating time	83
Figure 4.15 UPV versus degree of consolidation	86
Figure 4.16 Measuring the exposed area of the NM sample by Auto CAD program	88
Figure 4.17 Initial sorptivity versus consolidation degree.....	89
Figure 4.18 Secondary sorptivity versus consolidation degree	90
Figure 4.19 Relationship between consolidation degree and electrical conductivity.....	91
Figure 4.20 The effect of consolidation on electrical resistivity	92

Table of Tables

Table 2.1 A summary of different test methods used for crack assessment and their results	36
Table 2.2 Differences between this study and the previous research	50
Table 3.1 Concrete mixture proportions	53
Table 4.1 Concrete properties measured for Phases 1 and 2	70
Table 4.2 Concrete properties for Phase 3	70
Table 4.3 Average compressive strength and the coefficient of variation for different consolidation levels.....	85

1 INTRODUCTION

1.1 GENERAL DESCRIPTION

Considering the rapid rate of population growth and high industrialization speed of the world in the recent decades, an increasing demand for different types of new construction including roads, bridges, dams and buildings is inevitable. Concrete is known as the most common construction material used all around the world because of the numerous advantages it provides. The importance of concrete infrastructures is evident by its global use. However, the substantial environmental impact of concrete during its total life cycle, leads to a strong emphasis on sustainable industrial development. Disposal problem of concrete wastes, extensive energy consumption and considerable use of natural resources to produce raw material required for concrete production as well as the large amount of carbon dioxide emission associated with the manufacturing of Portland cement as one of the main concrete ingredients, makes it necessary to improve the sustainability of the construction industry.

Long term performance of concrete structures is significantly controlled by its strength and durability. In recent years, durability performance of concrete has attracted the interest of many researchers and has influenced many standard design codes. Increasing concrete durability minimizes the need for large maintenance, rehabilitation and reconstruction costs. Sustainability will be achieved by improving concrete durability and providing long service life structures.

Permeability is the most significant factor controlling concrete durability. Penetration of fluids and detrimental agents from the surrounding environment through concrete is associated with chemical and physical reactions which changes the concrete microstructure and results in premature deterioration. Carbonation, reinforcement corrosion and freezing and thawing action are the

primary causes of concrete deterioration due to the lack of permeation quality. Therefore, the ease with which water and aggressive ions can ingress through concrete; indicates its resistance against extreme environmental conditions which has a great impact on concrete durability. Thus, reducing the permeability of concrete is an effective way to preserve its desired integrity and serviceability.

Permeability reflects the concrete internal microstructure which in turn depends on the pore size distribution and connectivity of the pore network. Mixture constituents and water to cement ratio, degree of consolidation, degree of hydration and curing period are fundamental factors affecting the pore system properties of concrete. On the other hand, microcrack development as a result of physical and chemical interactions between concrete and environment plays an important role on changing the concrete microstructure (Stanish et al. 1997, Banthia et al. 2005 and Yang et al. 2006).

Microcracks can be formed in concrete structures due to several reasons including plastic shrinkage, drying shrinkage, temperature gradients, chemical attack, cyclic freezing and thawing and bleeding and segregation. Cracking will increase the mass transport process in concrete by providing an interconnected pathway for liquid and aggressive ion penetration through concrete and subsequent reduction of concrete durability. Therefore, investigating the causes of crack propagation in concrete and its effect on mass transport properties are of crucial importance for condition assessment of new and existing structures.

Faulty workmanship is believed to be another important reason for the lack of durability in concrete structures. Inadequate compaction is a common construction defect which appears in the surface of the concrete as honeycombing, voids and destructive air pockets which adversely affect concrete durability.

Over consolidation will also occur when the freshly mixed concrete is subjected to the excessive vibration time which results in segregation and sedimentation of the aggregates and induces the water rise towards the top surface of the concrete. Accumulation of the bleed water, weakens the concrete surface and increases the risk of plastic shrinkage cracking. The strength nonuniformity associated with the non-uniform distribution of the solid skeleton of concrete is another consequence of over vibration (Topcu et al. 2004 and Josserand et al. 2006).

On the other hand, concrete mixtures properly consolidated and cured remain more watertight and more durable under severe environmental conditions. Sufficient degree of consolidation is required to assure the quality of finished concrete. Therefore, more attention must be paid to provide satisfactory construction practices that fulfil the durability requirements (Mehta 2000).

1.2 RESEARCH OBJECTIVES

The main purpose of this study is to determine the influence of the most frequent defects including load induced cracking, thermal induced cracking and bleeding and segregation on the rate of mass transport properties of concrete by means of two standardized performance tests. This work attempts to illustrate the destructive effect of contaminant penetration through concrete with particular focus on water and chloride ion ingress and to evaluate the subsequent reduction of strength and durability of concrete.

The goal of this research was fulfilled in two stages. In the first part, sixty concrete samples with two different water to cement ratios were cast. Specimens were intentionally cracked under various levels of split tensile loading. Further, microwave heating was used for the next twenty-four specimens to induce shrinkage cracking by rapid drying of concrete samples for different durations. Ultrasonic pulse velocity was applied to quantify the extent of internal damage caused by both mechanical and thermal loading. Moreover, forty concrete samples were manufactured with different levels of vibrations to represent bleeding and segregation caused as a result of inappropriate degree of consolidation.

The second task of the project was intended to provide a quantitative assessment of the resistance of damaged concrete against penetration of aggressive agents using standard established methods. Water absorption (ASTM C1585) and bulk electrical conductivity (ASTM C1760) tests were conducted on all samples including the intact, control specimens to evaluate the permeability and durability of concrete.

1.3 ORGANIZATION OF THE THESIS

This thesis contains of five chapters as follows:

- Chapter 1 begins with the brief description of the concept of durability and the importance of microcrack propagation as well as consolidation on the rate of mass transport characteristics of concrete. The scope of the research is also explained.
- Chapter 2 consists of a detailed review of previous experiments regarding the effect of microcracks as well as the influence of insufficient consolidation on concrete properties including the compressive strength, ultrasonic pulse velocity, water permeability and electrical conductivity.
- Chapter 3 describes different test procedures and methods which were performed in the experimental program.
- Test results are summarized in chapter 4. Data obtained from laboratory measurements are discussed and compared with the findings of some relevant research.
- Chapter 5 presents the conclusion of this study as well as some recommended future works.

2 LITERATURE REVIEW

2.1 INTRODUCTION

This chapter includes a detailed overview of the available research concerning different causes of microcrack propagation in concrete and its effect on concrete durability. The influence of load induced cracking, thermal induced cracking, inadequate concrete consolidation as well as the over vibration on increasing the water permeability and the rate of chloride ingress through concrete has been explained.

2.2 CONCRETE DURABILITY

The growing evidence of durability problems in current concrete structures has become a serious concern in recent years more than ever before. It is much more economical to increase the durability of concrete materials rather than to allocate the large proportion of the available construction budget on extensive repair, rehabilitation and reconstruction costs.

The term ‘durability’ indicates the ability of hardened concrete to maintain its original quality and serviceability against external physical and chemical attacks over the life time of the structure. Nowadays, it is believed that durability affects the integrity and stability of concrete structures as much as strength and mechanical properties do. So, lack of sufficient durability is responsible for premature concrete deterioration (Mehta and Monteiro 2006).

Durability is directly dependent on permeability and porosity of concrete. The rate of destructive reactions in concrete can be controlled by improving its penetration resistance. An impermeable pore structure protects concrete from the ingress of aggressive substances and increases concrete’s longevity in harsh environments.

Water is the major substance involved in the most frequent deterioration mechanisms in concrete. Increasing the moisture content of concrete accelerates the rate of deterioration in different ways. For example, the high hydraulic pressure produced by freezing of water in concrete pores during the freeze and thaw process causes destructive expansion which results in cracking and reduces concrete durability. Reinforcement corrosion initiates when water contaminated by chloride ion passes through the concrete cover and reaches to the level of steel reinforcement thus destroying the protecting passive film. Reinforcement corrosion also occurs due to the reaction between carbon dioxide and calcium hydroxide in the presence of water which lowers the pH of concrete and dissolves the oxide layer around the steel surface. Alkali silica reaction occurs between aggregates containing reactive silica and alkali hydroxides of concrete pore solution to form alkali silica gel which swells upon contact with moisture. Cracks are formed in all these cases due to expansive pressure. Correlation between the amount of absorbed water by concrete and all mentioned destructive processes is well established by Basheer et al. (2001).

According to Wiens et al. (1997), even the presence of small surface microcracks can greatly increase the facility for water and deicing salts to penetrate through concrete and intensify concrete deterioration. Therefore, durability measurements based on undamaged, intact samples provide misleading evaluation of the real behavior of concrete structures in the field which cannot be used as a reliable representative for lifecycle prediction models.

Several standard test methods have been established to measure concrete durability either directly or indirectly, among which chloride ion permeability and the rate of water absorption referred to as sorptivity are considered as the most promising tests for durability performance assessment which were used in the current study.

2.3 DIFFERENT MASS TRANSPORT MECHANISMS IN CONCRETE

Concrete resistance against an aggressive environment is greatly dependant on the rate of movement of deleterious substances through concrete as well as different factors controlling this rate. In order to determine how cracking changes the concrete microstructure and affects the mass transport properties of concrete, it is important to study different mechanisms by which liquid and aggressive ions can penetrate in to concrete. Different transfer processes through concrete are classified as absorption, permeation and diffusion that are directly influenced by the presence of microcracking (Samaha and Hover 1992, Basheer et al. 2001 and Castro et al. 2011).

2.3.1 Absorption

Water absorption or sorptivity is defined as the water movement through porous unsaturated materials due to the capillary suction forces. The time dependency of one-dimensional water flow into concrete has been presented as the following equation by Hall (1987):

$$i = A + St^{1/2} \quad \text{[Equation. 2.1]}$$

where:

i: Cumulative volume of water absorbed per unit area of inflow surface (mm)

A: Constant term reflects the initial surface disturbance (mm)

S: Sorptivity of material (mm/s^{0.5})

t: Elapsed time (s).

Water absorption test is a simple and reliable method which provides important information needed to assess concrete durability. Pore system characteristics including porosity, pore size distribution, pore connectivity and tortuosity are the main factors controlling the amount of

concrete water absorption. Also, the moisture content of concrete has a great influence on sorptivity since the capillary absorption will increase as the relative humidity decrease (Hoseini et al. 2009, Shahroodi 2010 and Castro et al. 2011).

Sorptivity can be measured by laboratory tests either on laboratory molded cylinders or on concrete cores drilled from existing structures. In-situ sorptivity tests can also be used as non-destructive methods to determine the rate of water absorption in the field.

ASTM C 1585 is the standardized laboratory test method frequently used to measure the rate of water ingress through hydraulic cement concrete by means of capillary suction force exerted by the pore structure, when only one side of the sample is exposed to water (Figure 2.1). Sorptivity is determined by measuring the incremental mass changes of the specimen over the specific time intervals. ASTM C 1585 indicates the rate of water absorption i , using the following relationship:

$$i = \frac{m_t}{a.d} \quad \text{[Equation. 2.2]}$$

In which:

i = Absorption (mm)

m_t = Changes in the specimen mass at time t (g)

a = Exposed area of the specimen (mm²)

d = Density of the water (g/mm³).

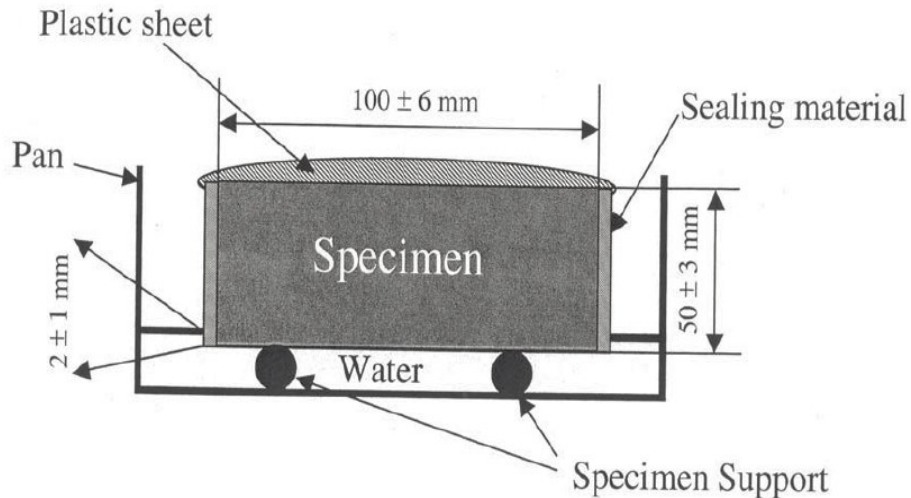


Figure 2.1 Schematic of the sorptivity test (ASTM C 1585-04)

The typical results of cumulative water absorption, I , are plotted against the square root of the time as shown in Figure 2.2. The rate of water absorption, known as sorptivity, can be obtained by the slope of the line best fitted to this curve using the least-square linear regression analysis. This graph includes two linear parts corresponding to the short term (initial) and long term (secondary) water absorption.

Data recorded for the cumulative water absorption in the first 6 hours are used to calculate the initial sorptivity. Initial sorptivity represents the rapid filling of cracks and larger pores upon contact with water. Secondary sorptivity describes the slower rate of gel pores saturation based on the data between 1 and 8 days (Yang et al. 2006)

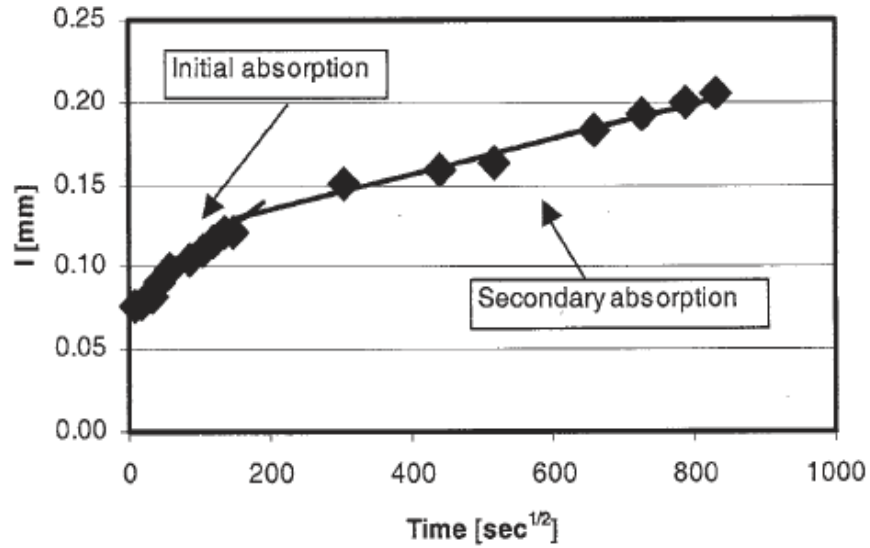


Figure 2.2 Typical water absorption test data (ASTM C1585-04)

In addition to the ASTM Standards C1585 and C642 which are laboratory techniques, initial surface absorption test (ISAT), Standpipe absorptivity, Figg and Autoclam tests are the most common in-situ test methods for measuring the water absorption of concrete (Basheer et al. 2001).

2.3.2 Permeability

The passage of fluid through saturated material under the pressure differential is described by permeability. The uniaxial water movement through a saturated porous material like concrete can be modeled by Darcy's law as shown in Equation 2.3 in which K is the coefficient of permeability which depends on the type of concrete and dh is the differential head across the passage length of dL (Basheer et al. 2001). There are no standardized water permeability tests for concrete.

$$u = -K(dh / dL)$$

[Equation. 2.3]

2.3.3 Diffusion

Diffusion is the process that represents the passage of an agent due to a concentration gradient. Diffusion occurs with the random movement of particles and ions from the higher concentration regions toward less-concentrated parts. Diffusion is the principal way for chloride ion to penetrate through concrete. Generally, three different types of ionic diffusion test methods are commonly used as follows: (Basheer et al. 2001)

1. Steady state migration test: is a simple and slow process in which a concrete slice is placed between a cell containing ion solution and another cell free of chloride solution. This allows the mass transfer through the concrete section under the gradients of concentration. The diffusion coefficient is measured by Fick's first law as soon as a steady state flow is reached (Stanish et al. 1997):

$$J = -D \frac{dc}{dx} \quad \text{[Equation. 2.4]}$$

where:

J: flux of chloride ions ($\text{mol.s}^{-1}.\text{m}^{-2}$)

c: Concentration of chloride ion (mol/m^3)

D: Diffusion coefficient (m^2/s)

x: Position variable (m)

2. Non steady state migration test: is a uni-dimensional penetration in which a specimen with only one unsealed surface is immersed in a chloride ion solution for a specific time. Since the concentration of the chloride ion in concrete elements normally changes with time, the

non-steady state condition is the more useful form of diffusion which is controlled by Fick's second law (Stanish et al. 1997 and Sillanpaa 2010).

$$\frac{\partial c}{\partial t} = D \frac{\partial^2 c}{\partial x^2} \quad \text{[Equation. 2.5]}$$

where:

c: Concentration of chloride ion (mol/m³)

D: Diffusion coefficient (m²/s)

x: Position variable (m)

t: time (s)

3. Electrical migration test: this method relies on accelerating the movement of chloride ion under an electrical potential gradient. This is a short term test that has been used in this research to evaluate the resistance of concrete against the chloride ion ingress. This method is explained in details in chapter 3.

2.4 DIFFERENT CAUSES OF CRACKING IN CONCRETE

Concrete is a heterogeneous material composed of different dissimilar ingredients and its resistance against cracking and aggressive conditions depends on the properties of its multiphase materials. The influence of internal cracking on concrete behaviour in terms of strength and durability characteristics has been well recognised. Thus understanding the origin of formation, propagation and stabilization of various types of microcracks is of crucial importance in order to investigate the effect of cracking on mass transport mechanism in concrete structures.

Concrete susceptibility to crack initiation increases as the number of voids and initial defects increase. Cracking occurs during all stages of concrete service life as a result of many factors which can be generally classified as two main groups:

1. Cause of cracking before hardening
2. Cause of cracking after hardening.

2.4.1 Cracking occurred before hardening

Although deterioration of concrete structures occurs during a long term process, the presence of early age damage can reduce the loading capacity of concrete and make it more vulnerable to further chemical and physical attack and accelerate the rate of deterioration (Yang 2004).

Soon after placing and finishing the concrete when it is in the plastic state, crack developments can start at the surface of the fresh concrete due to the following reasons (Kelly 1981 and Menzel 1954):

2.4.1.1 Constructional movement

Cracking occurs when the tensile stress which results from restrained movement between the concrete and subgrade or movement between the concrete and formwork, exceeds the tensile strength of concrete.

2.4.1.2 Settlement shrinkage

Plastic settlement cracking occurs in the first few hours after placing and finishing the concrete surface due to the settlement of concrete around reinforcement bars, aggregates or other

obstructions which may result in cracking. Insufficient compaction intensifies the degree of settlement shrinkage damage.

2.4.1.3 Plastic shrinkage

Rapid moisture loss from the surface of fresh concrete causes plastic shrinkage. Plastic shrinkage occurs at an early age when concrete has not yet achieved sufficient rigidity and strength. Shrinkage occurs when the rate of moisture evaporation from the surface of freshly placed concrete is faster than the rate of bleed water due to the inadequate curing procedure. Tensile cracking develops when the movements related to the volume changes of the concrete surface are restrained by the inner layers. These V shape cracks are relatively shallow and wide (2-3 mm) in the surface of the concrete with random pattern and the length varying from 5 cm to a few meters. Plastic shrinkage cracking is more probable in concrete elements with high surface area such as pavements and slabs (Yang 2004).

2.4.1.4 Faulty workmanship

Construction practices have a great influence on the quality of finished concrete. Improper construction joints facilitate the leakage of water contaminated with chloride and aggressive ions through concrete elements which increase the risk of freeze and thaw deterioration. Highly porous concrete manifested in the forms of bug holes, air voids and honeycombing result from poor compaction and consolidation are one of the main reasons for premature concrete deterioration. On the other hand, segregation due to over vibration is another construction defect which weakens the bond between aggregate and paste and prevents sufficient contact between concrete and steel rebars (Rasheeduzzafar et al. 1989).

2.4.2 Cracking occurring after hardening

Concrete is vulnerable to a number of problems even after setting and hardening. The most important causes of cracking and damage of concrete over time are as follows:

2.4.2.1 Chemical attack

Steel reinforcing embedded in different parts of concrete structures are initially protected from corrosion by the inherent alkaline environment of the cement matrix. Steel corrosion occurs mainly because of carbonation and chloride attack. Penetration of the chloride ion in the presence of water and oxygen will decrease the pH of the concrete and deteriorate the passive oxide film surrounding the reinforcement and consequently corrosion initiates. The rust formation resulting from the corrosion process occupies a greater volume (up to four times) in comparison with the original steel bars. This expansion produces tensile stresses which form a series of cracks parallel to the surface of the concrete. If the concrete cover depth is not sufficient, crack development results in spalling and separation of concrete (Shokouhi et al. 2011).

Alkali Aggregate Reaction (AAR) is another destructive chemical reaction that occurs in two possible forms:

1. Alkali Silica Reaction (ASR) involves the reaction between the active mineral components of aggregates, such as non-crystalline forms of silica, and sodium, potassium and calcium hydroxides in the pore solution to produce viscous alkali-silica gel that swells while absorbing water. The expansive pressure caused by increasing the volume of silicate gel will induce network cracking, closed or spalled joints and structure displacement.
2. Alkali Carbonate Reaction is another type of AAR happens due to the reaction between dolomitic rocks and highly alkaline hydroxides in cement matrix. The expansive pressure

results from the reaction product leads to cracking and concrete deterioration (Huang 2006).

2.4.2.2 **Drying shrinkage**

Drying of the concrete surface at later stages also causes cracking. If the volumetric changes of concrete layers resulting from moisture loss are restricted by internal or external obstruction, tensile cracking forms through the concrete matrix with a radial pattern. Drying shrinkage cracking increases concrete permeability and makes it less durable.

Drying shrinkage is affected by many factors such as water to cement ratio, the amount of cement and different types of admixtures, shape, texture and size of aggregate, concrete geometry, wind velocity, air temperature and relative humidity. According to the Highway Research Board report, drying shrinkage of hardened concrete is the most frequent cause of cracking and consequent decrease in the durability of highway structures in Canada and United States (Kelly 1981).

2.4.2.3 **Thermal variation**

Early age cracking develops due to the thermal stresses induced by extreme temperature variation across the concrete section during the cement hydration process. In general, between 5 to 9°C temperature rise is expected from the hydration reaction for every 45 kg of Portland cement (Kosmatka and Panarese 2002). Released heat of hydration will increase the internal temperature of concrete to as high as 80°C while it dissipates rapidly at the surface. Since the contraction of cooler layers of concrete is restraint for the hot interior parts, tensile cracking is generated.

After hardening, different parts of a concrete element may heat or cool at different rates and different degrees upon exposure to extreme weather conditions. The temperature gradients due to the different thermal coefficients of expansion and contraction between hydrated cement paste

(HCP), fine and coarse aggregates result in restraint volume changes which produce tensile cracking. The more massive the concrete, the higher is the susceptibility of thermal cracking.

2.4.2.4 Freeze and thaw action

Freezing and thawing cycles can be considered as the most wrecking effect of weathering. Water penetrates through concrete and saturates the internal pores of aggregate and cement paste. When the concrete temperature drops below 0°C, water starts freezing and converting to ice crystals which expand and occupy almost 9 percent greater volume. Cracking appears parallel to the longitudinal and transverse joints, when the internal pressure results from repetitive cycles of freezing and thawing exceeds the tensile strength of concrete.

2.4.2.5 Overloading

Cracking is the first sign of damage as a result of over-loading which is initiated in the vicinity of the applied stress and will propagate throughout the concrete depth. When concrete structures are overstressed, reaching to the ultimate strength, their loading capacity decreases and results in structural failure. Shear, flexural and tensile cracking are the most common types of defects under loading. Cracking also develops under the effect of creep, fatigue, impact and vibration loads (Huang 2006).

2.5 FRACTURE OF PLAIN CONCRETE UNDER MECHANICAL LOADING

The region between the aggregates and the cement paste in concrete is called interfacial transition zone (ITZ). The high porosity and heterogeneity of the ITZ makes it the weakest region in the concrete system which is highly prone to crack propagation even prior to the external loading (Hearn 1999). Initial flaws and microcracks are present in concrete due to the volume changes and temperature gradients during the setting and hydration process (Santiago et al. 1973). Pre-existing

bond cracks around coarse aggregates begin to increase in number and connectivity and finally extend into the mortar upon exposure to incremental loading. When reaching a critical stress level, a rapid increase in concrete volume as a result of microcrack branching through cement matrix causes serious deformations and results in concrete fracture.

According to Meyers et al. (1969), two types of microcracking can occur under loading:

1. Bond cracks that are observed at the aggregate-paste interface, and
2. Mortar cracks which form within the paste matrix.

Bond cracking frequently occurs in the aggregate-paste interface due to the strain and strength incompatibility and high stress concentration at this region which makes a weak bond between mortar and coarse aggregate. The high water to cement ratio that exists close to the larger particles of aggregate is responsible for the high porosity of the interfacial transition zone. Thus, a large proportion of randomly oriented bond cracking initiates between cement paste and aggregate before exposure to external loading as a result of volumetric changes associated with settlement, drying shrinkage, bleeding and segregation. These interfacial cracks remain stable on increasing the load up to 30 % of ultimate strength. However, the length and number of bond cracking increase as the load rises from 30 % to 70% of the peak load corresponding to the initial non linearity of the stress-strain curve. Beyond 70% of ultimate strength for normal strength concrete, unstable mortar cracking will propagate and join adjacent bond cracks thus reducing the concrete stiffness, making the stress-strain curve horizontal and resulting in failure.

Later, a more comprehensive crack classification was done by Carrasquillo et al. (1981) in which cracking is divided in to three main types:

1. Simple cracks
2. Combined cracks type I
3. Combined cracks type II

Simple cracks are single, isolated cracks formed in the aggregate-mortar interface at the primary stages of applying load which remain stable under constant loading. Mortar cracks start to form at higher load levels, bridging to the existing simple cracks to form unstable combined cracks. Combined cracks type I, consist of one mortar crack and one bond crack or more commonly it is the combination of one mortar crack which connects two bond cracks to each other. Type II cracks also called complex combined cracks involve at least two bond cracks and two mortar cracks which will propagate even under constant loading and result in concrete failure. Development of type II combined cracks is noticeable at 70 % and 90 % of the peak load for normal and high strength concrete, respectively. Figure 2.3 shows different types of cracking.

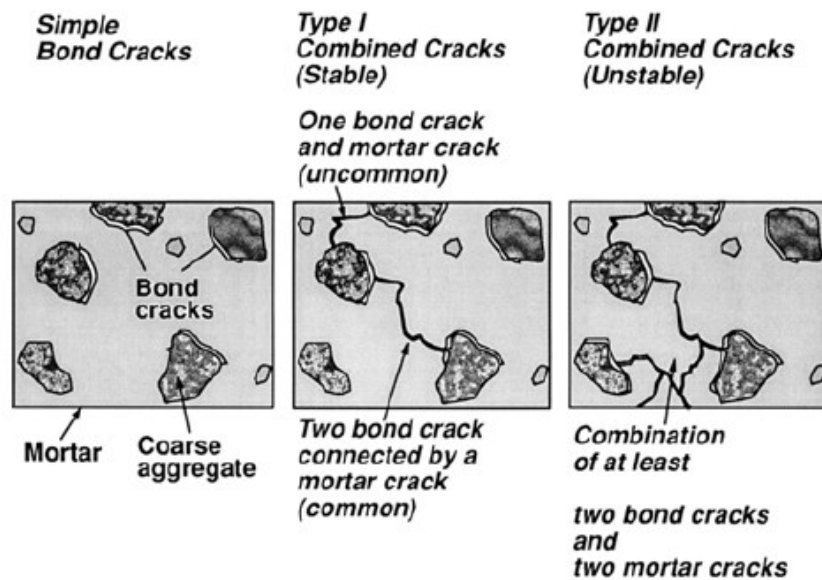


Figure 2.3 Different types of cracking (Heran 1999)

2.6 METHODS FOR MICROCRACK DETECTION IN CONCRETE

Development of reliable inspection methods is required for quality assessment and predicting the remaining service life of concrete structures. The increasing rate of infrastructure deterioration due to the stress concentration, erosion and environmental attack leads to relatively large repair and rehabilitation expenses all around the world. Thus, early detection of damage and identification of the symptoms of distress and anomalies in concrete is important before the serious forms of deterioration become evident. Structural health monitoring in addition to the regular maintenance strategies are combined to insure the long term performance of concrete and its structural integrity and loading capacity (Acciani et al. 2010 and Shah and Ribakov 2012.).

As a purpose of this research, microcrack detection and quantification was necessary in order to find how the existence of internal damages resulting from mechanical loading affects the mass transfer properties of concrete. Scanning electron microscopy, X-radiography and non-destructive testing (NDT) methods are the most commonly used diagnostic techniques to detect the extent of damage in concrete. NDT seems to be more attractive for both laboratory measurements and in situ investigations due to the simple, quick and effective condition assessment without impairing the function of concrete element (Loo 1992 and Yang 2004).

Ultrasonic pulse velocity (UPV) is a non-destructive technique which has been successfully applied for more than 6 decades to identify the presence of under surface flaws and defects. UPV provides valuable information about the uniformity and quality of hardened concrete. This approach enables the indication of internal voids and microcracks and determines the position of heterogeneities and discontinuities. Ultrasonic inspection of concrete structures reveals the onset of damage and degradation prior to the significant reduction of concrete strength and durability. Thus, it can provide a threshold limit for design criteria in concrete structures. UPV can also be

used for monitoring the changes in the material properties over time (Malhotra and Carino 2004 and Mahmood 2008).

As shown in Figure 2.4, the UPV test setup consists of one generator transducer and one receiver transducer connected to the concrete surface to measure the time for the pulse traveling through a known distance.

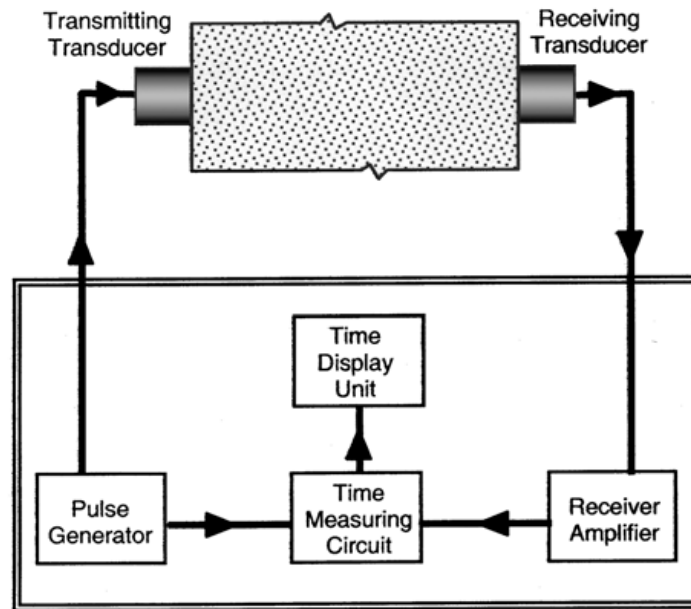


Figure 2.4 Schematic of pulse velocity apparatus (ASTM C 597-09)

Ultrasound pulse propagation will be scattered when encountering heterogeneities. Therefore, variation in the velocity of longitudinal elastic waves shows the presence of cracking and internal deficiencies. The delay in the arrival time of the pulse wave to the receiver is a significant index for surface breaking. Generally, lower transmission times represent better quality conditions (Ramamoorthy et al. 2004 and Mahmood 2008).

Jones (1951) applied the UPV method to detect the onset of cracking in concrete samples subjected to tensile and compressive loading. A significant decrease in the velocity of waves was observed

when measuring perpendicular to the direction of loading while the changes in the velocity were negligible in the axial direction. This suggests that cracking propagates parallel to the loading direction when exposed to compressive stresses.

In 1970, Shah and Chandra investigated the stress effect on the fracture mechanism of concrete and paste by means of ultrasound wave velocity. Samples were subjected to both cyclic and sustained compressive loading ranged from 60 to 90 % of the maximum capacity. Crack growth under loading was proved by significant decrease in the pulse velocity near failure (Shah and Chandra 1970).

In the study performed by Raju (1970), the change in the sonic pulse velocity was used to detect the microcrack propagation in high strength concrete under static and cyclic compressive loading with the purpose of predicting the remaining fatigue life of the damaged concrete. The relation between different compressive stress levels and UPV variations is depicted in Figure 2.5. Although UPV remains relatively constant at low stress levels, a significant reduction in the pulse velocity could be observed between 68 to 75% of the peak strength. This was followed by the average decrease of 9% in the pulse velocity in the transverse direction at failure.

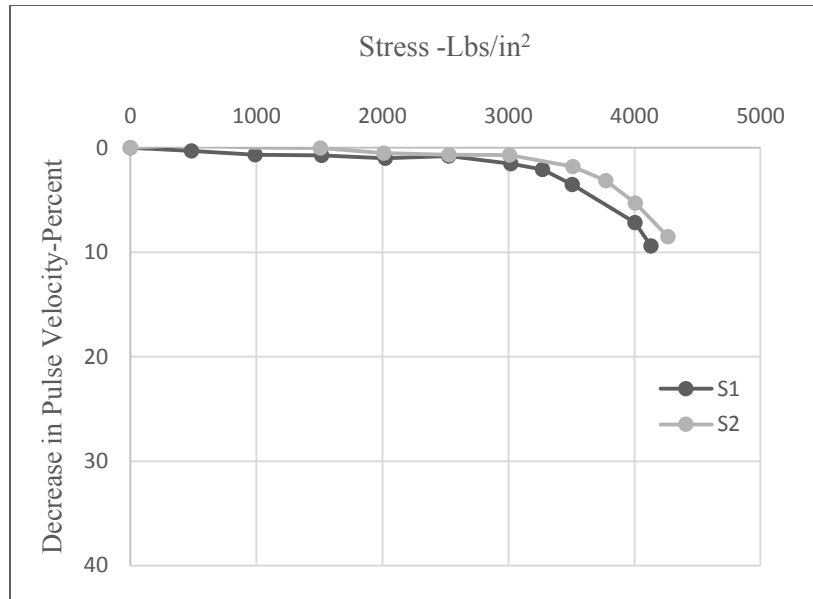


Figure 2.5 Decrease in UPV versus different compressive stress levels (after Raju 1997)

In the study conducted by Knab et al. (1983), cracks of 0.05 mm thickness were induced in concrete cubes at different depths of 19, 38 and 57mm. Both ultrasonic pulse velocity and amplitude were measured perpendicular to the crack plane with the frequencies of 150 and 54 kHz. The presence of cracks located at the two greater depths was reliably indicated with both methods. However, they found that pulse velocity is a more sensitive parameter for crack detection. The transducer frequency did not have a noticeable effect on these results.

Variation of ultrasonic pulse velocity under repetitive compressive loading has been utilized to indicate microcrack propagation in concrete and mortar with different water to cement ratios (Wu and Lin 1998). The selected cyclic loading levels were 50, 70 and 80% of the ultimate strength. Pulse velocity decreases by increasing the number of load cycles and microcrack growth around aggregates. They found the greater stress-velocity relation in concrete than mortar samples.

2.7 EFFECT OF CRACKING ON CONCRETE DETERIORATION

In addition to the hydrated cement paste (HCP) and solid phase, concrete contains a pore system with different types of voids which can be classified as follows (Mehta and Monteiro 2006):

- Small gel pores ranging from 0.5-10 nm. The destructive influence of these micropores on strength and durability of concrete is negligible.
- Capillary voids, with the dimension of 10 to 50 nm, have an important effect on drying shrinkage. Capillary voids with an average radius larger than 50 nm, which are considered as macropores, are responsible for strength reduction and primarily responsible for durability issues, and finally,
- Air voids which are accidental voids entrapped in concrete during mixing as well as the entrained air voids which are deliberately added to the concrete in the form of admixtures.

In well-hydrated and well-compacted concrete with low water to cement ratio, the internal pore system existing in concrete is the only potential way for water and dissolved ions to penetrate. But microcracks, referred to as fine cracks with a width varying from 10 to 100 microns, can also be induced in concrete due to several reasons that were mentioned before. Microcracks are significantly larger in size compared to the typical voids and capillaries in concrete. Thus, they have more potential to connect to each other and modify the concrete microstructure in a way to increase mass transport characteristics of concrete which results in further deterioration. In general, crack propagation provides interconnected flow channels that increase the permeability of concrete and facilitates the movement of water, gases and dissolved chemical ions through the concrete structure by means of diffusion, absorption and permeation or a combination of two or more mechanisms.

The effect of cracking on concrete permeability has been the subject of many investigations so far. According to the previous research, there is a direct correlation between concrete permeability and mechanical degradation.

Ludrija et al. (1989) introduced a simple apparatus to measure the water permeability of concrete under atmospheric pressure. Their results indicated that although development of noticeable load-induced damage was evident from ultrasonic pulse velocity (UPV), the concrete coefficient of permeability did not undergo significant increase even up to 80 % of ultimate strength.

According to Kermani (1991), 40% of the compressive strength is the threshold stress level beyond which the water permeability of ordinary Portland cement concrete, air entrained concrete and concrete containing fly ash will increase rapidly. Further, this threshold level was estimated to be 50% by Bhargva and Banthia (2006) who obtained the water permeability of concrete under loading. (Figure 2.6)

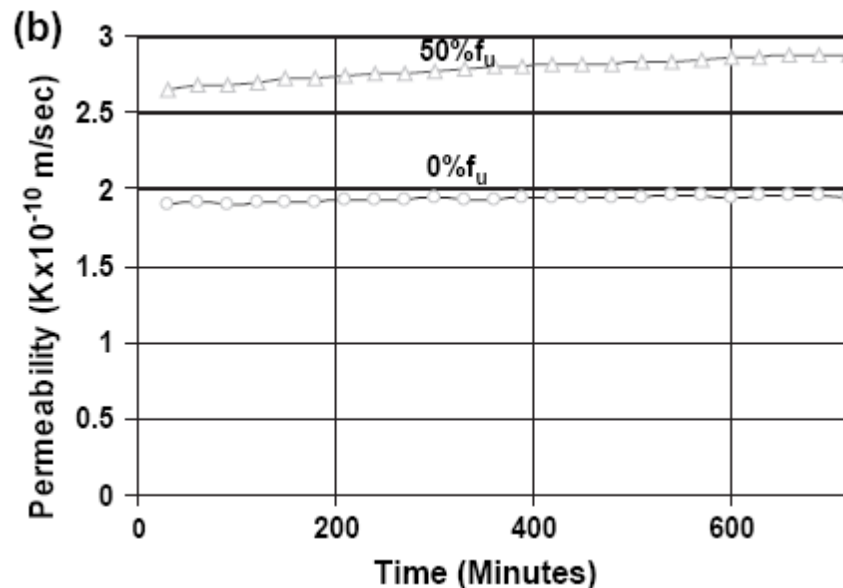


Figure 2.6 Coefficient of permeability for stressed and unstressed specimens at 7 days (Bhargva and Banthia 2006)

In the study conducted by Samaha and Hover (1992), concrete cylinders were subjected to different uniaxial compressive stress levels including 40%, 75% and 100% of the peak strength in order to investigate the influence of load-induced cracking on the rate of water absorption and rapid chloride permeability of concrete. Also, the Neutron Radiography technique was used to visualize the extent of internal damage. Although cumulative crack length increased by increasing the compressive load levels, they did not notice any increase in the chloride ion transport through concrete subjected to stress levels below 75% of the ultimate strength. This was accompanied by 20% increase in the total charge passed at higher loads. On the other hand, the maximum percentage of concrete water absorption performed based on NCHRP 244 report, was achieved at 75% of peak strength. Results can be observed in Figures 2.7 and 2.8.

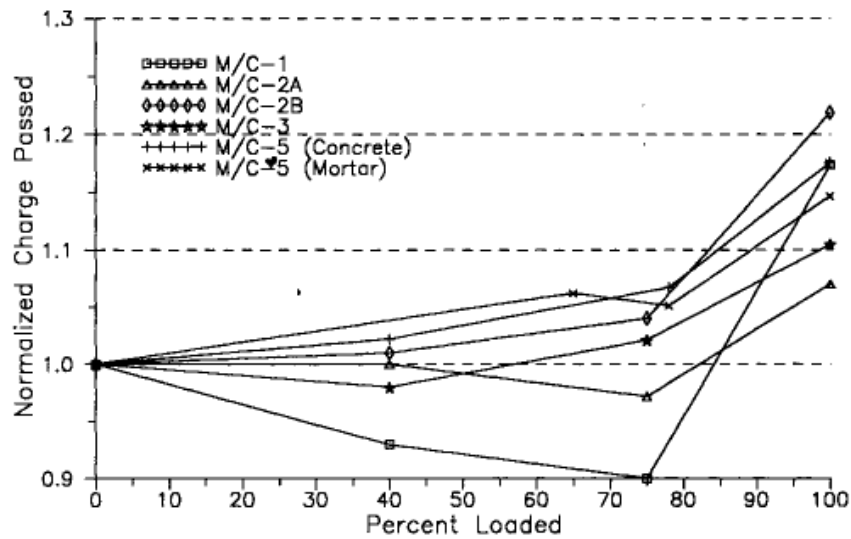


Figure 2.7 Normalized charge passed against compressive stress levels (Samaha and Hover 1992)

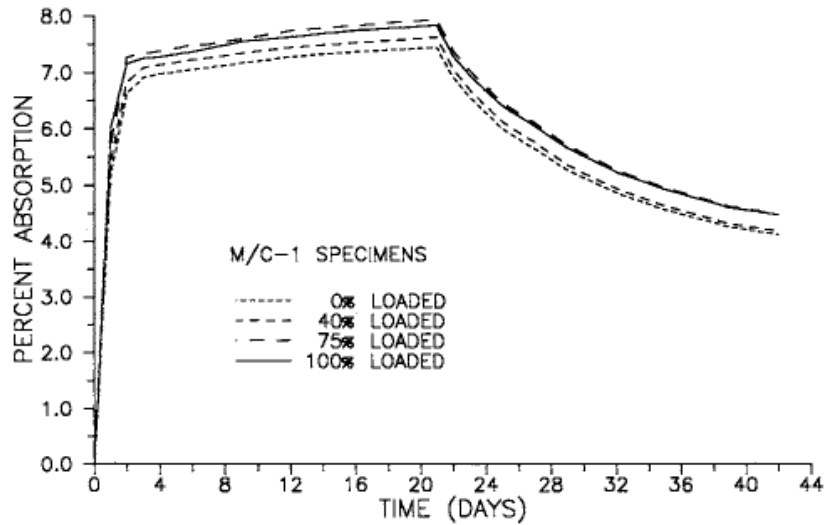


Figure 2.8 Water absorption versus time for different load percentages (Samaha and Hover 1992)

Further, Sugiyama et al. (1993) observed a sharp increase in the chloride ion ingress through concrete samples subjected to sustained compressive loading greater than 65% of ultimate strength. Saito and Ishimori (1995) showed that increasing the static compressive loading from 30% to 90% of the maximum strength has only little influence on chloride permeability of concrete measured according to AASHTO T277 method (Figure 2.9). However, cyclic loading above 60% of ultimate strength results in a noticeable increase in chloride permeability of concrete.

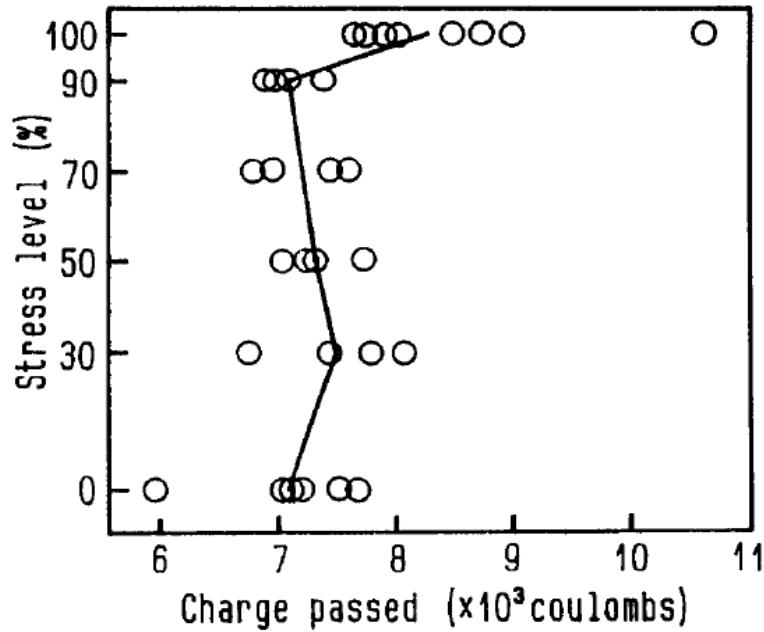


Figure 2.9 Charge passed against different stress levels (Saito and Ishimori 1995)

Gerad et al. (1996) observed that water permeability of prismatic concrete samples subjected to direct tension is greatly dependent on the crack density and crack opening in the range of 0.1 μm to 0.1 mm. Wang et al. (1997) also determined the effect of tensile induced cracking on water permeability of concrete. Cracks of predetermined widths were generated using feedback-controlled splitting test in concrete discs of 25 mm thickness. While the effect of crack width less than 50 microns on concrete permeability was negligible, they found a rapid increase in water flow for crack opening displacement rising from 50 to 200 microns under loading. A comparison was made between the effect of shrinkage-induced cracking and load-induced cracking on the mass transfer properties of concrete (Hearn 1999). Concrete cylinders of five different water to cement ratios were subjected to uniaxial compressive loading with desired stress levels of 30, 50, 70 and 80% of the peak strength with the duration of 10 minutes. Samples were then evaluated by acoustic emission and ultrasonic pulse velocity before performing the water permeability test. Results indicated that water permeability and ultrasonic pulse velocity are insensitive to short term

compressive stress loading below 80% of ultimate strength (Figure 2.10). The reason is believed to be due to the significant crack recovery upon unloading.

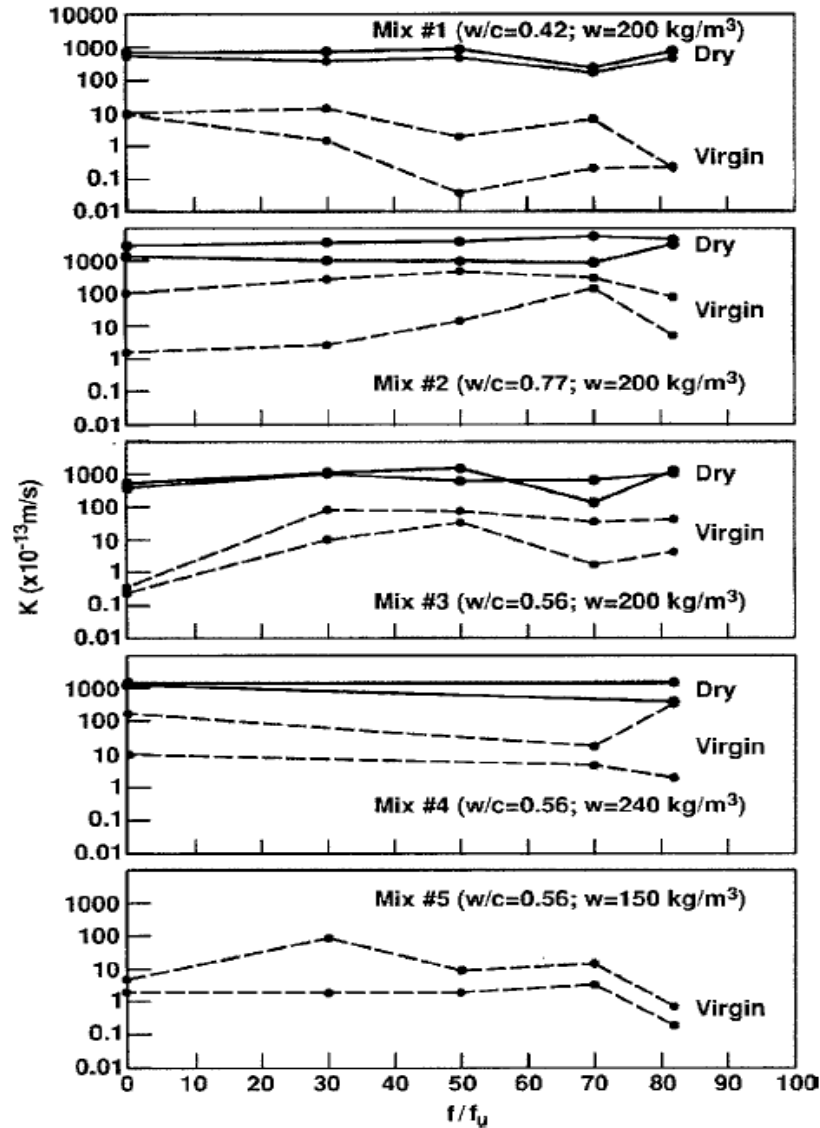


Figure 2.10 Coefficient of permeability versus stress levels (Hearn 1999)

Water and chloride permeability of normal strength and high strength concrete subjected to tensile stress were measured by Aldea et al. (1999). Crack opening displacements ranging from 50 to 400 μm were generated under a Brazilian test configuration. They found 64% and 56% decrease in

crack width after unloading for high and normal strength concrete, respectively. As expected, normal strength concrete is more permeable than high strength concrete particularly for crack width greater than 200 μm . As can be observed from Figures 2.11 and 2.12, water permeability increased dramatically as crack width grew while there was not any direct trend between crack width and chloride ingress in to the concrete. So, it was concluded that water permeability is more sensitive to mechanical damage. Furthermore, they found that water permeability is strongly influenced by crack width while measured under loading (Aldea et al. 2000).

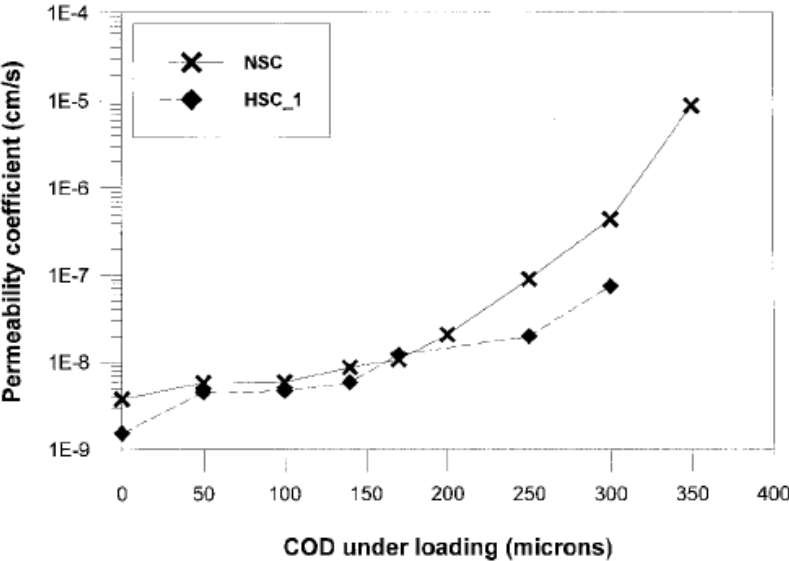


Figure 2.11 Water permeability versus crack opening displacement (Aldea et al. 1999)

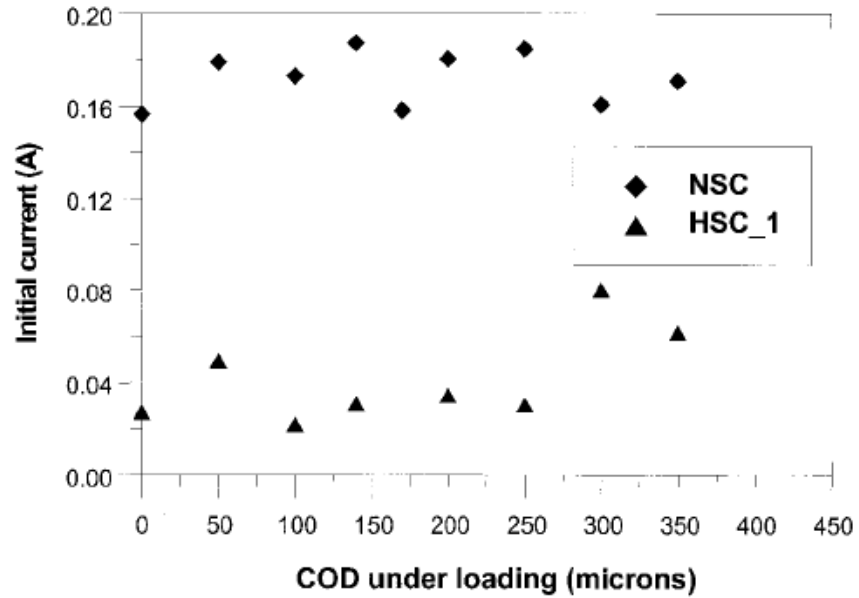


Figure 2.12 Initial current versus crack opening displacement (Aldea et al. 1999)

Lim et al. (2000) also determined the effect of load induced cracking on electrical charge passed through concrete using ASTM C1202 test method. Their study involved microscopic examination of concrete samples which were uniaxially loaded from 30 to 95% of the compressive strength (f'_c), to measure the microcrack characteristics such as crack area. Significant crack recovery could be observed below 70% of ultimate strength upon unloading (Figure 2.13). This is probably the reason for the negligible change that occurred in the chloride permeability of concrete below the critical stress level of $0.8f'_c$. As shown in Figure 2.14 chloride permeability is greatly increased when exceeding the critical stress level.

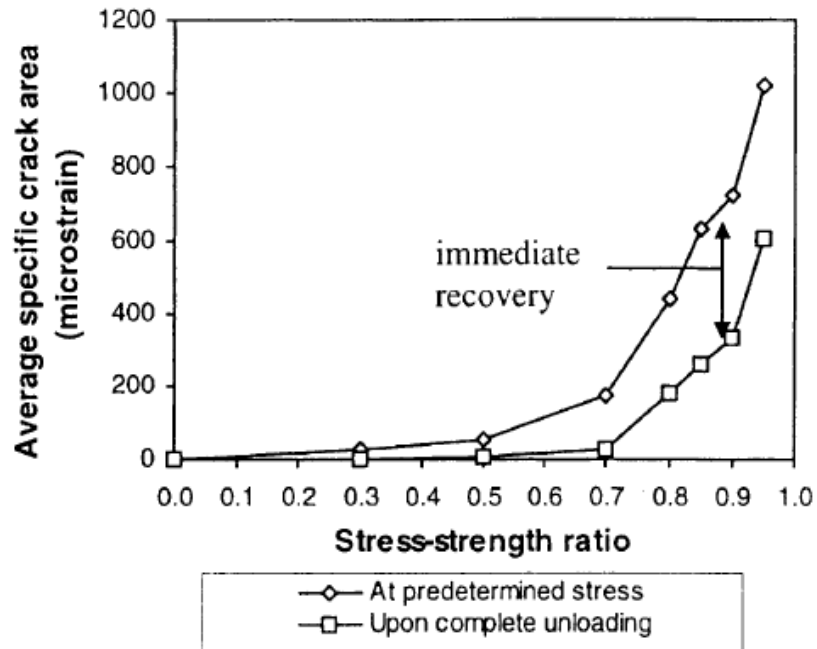


Figure 2.13 Average crack area before and after loading (Lim et al. 2000)

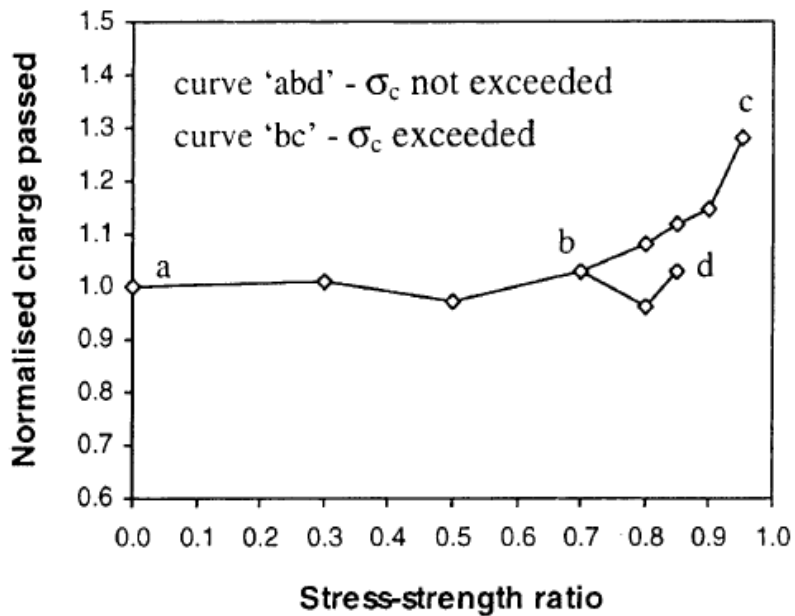


Figure 2.14 RCPT results for different stress-strength ratios (Lim et al. 2000)

Yang et al. (2006) compared the effect of local damage results from mechanical loading with the effect of global damage results from cyclic freezing and thawing, on mass transport properties of concrete. Acoustic emission (AE) and scanning electron microscopy (SEM) were used to identify the degree of internal damage and crack pattern respectively. Although two or three times increase in transport properties of concrete subjected to freeze and thaw process was reported, water absorption and electrical conductivity of concrete beams were insensitive to the localized and disconnected cracking occurred under tensile loading even at 90% of the ultimate load. Results are depicted in Figures 2.15 and 2.16.

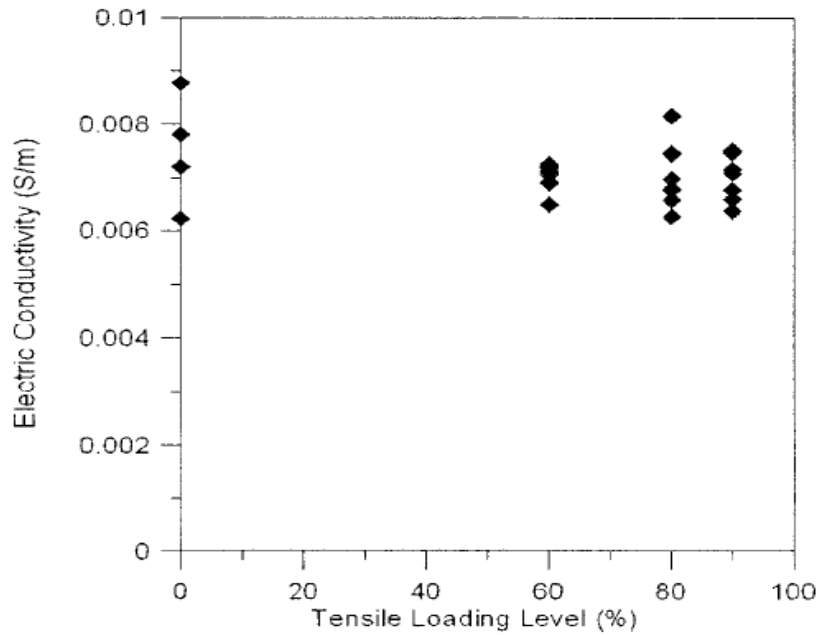


Figure 2.15 Electrical conductivity against different stress-strength ratios (Yang et al. 2006)

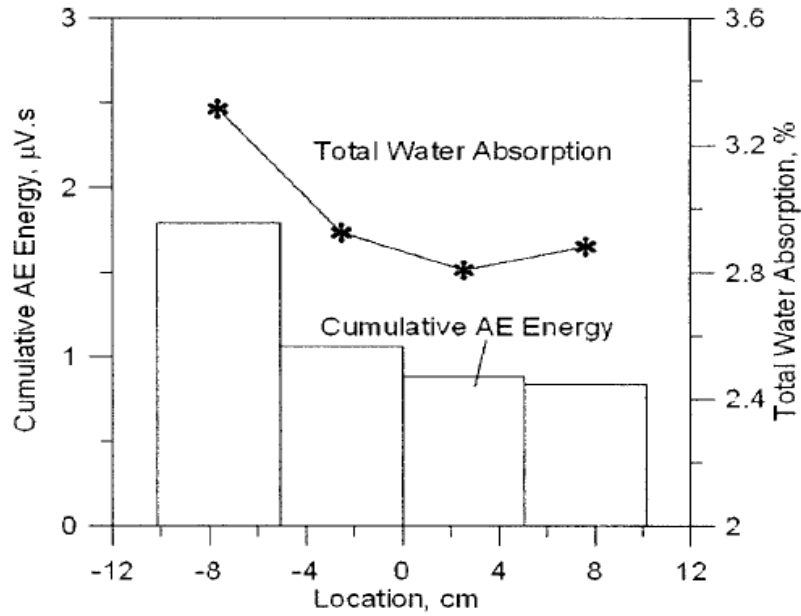


Figure 2.16 AE versus water absorption at 90% of tensile strength loading (Yang et al. 2006)

Yoon et al. (2007) applied rapid chloride migration test (RCM) to analyse the effect of tensile induced cracking on chloride permeability. It was shown that only crack width higher than 0.012 mm will lead to a significant increase in chloride penetration towards concrete.

2.7.1 Summary

The results of different test methods used for crack assessment by previous research are summarized in Table 2.1:

Table 2.1 A summary of different test methods used for crack assessment and their results

Reference	Test method	Critical load or crack width
Ludrija et al. (1989)	Water permeability test	80% of the compressive strength
Kermani (1991)	Water permeability test	40% of the compressive strength
Bhargva & Banthia (2006)	Water permeability test	50% of the compressive strength
Samaha and Hover (1992)	Chloride permeability test Water absorption test	75% of the compressive strength 75% of the compressive strength
Sugiyama et al. (1993)	Chloride permeability test	65% of the compressive strength
Saito and Ishimori (1995)	Chloride permeability test	Above 90% of the compressive strength
Gerad et al. (1996)	Water permeability test	0.1 μm to 0.1 mm
Wang et al. (1997)	Water permeability test	50 to 200 microns
Hearn (1999)	Water permeability test	Above 80% of the compressive strength
Aldea et al. (1999).	Water permeability test Chloride permeability test	Above 200 microns Above 400 microns
Lim et al. (2000)	Chloride permeability test	80% of the compressive strength
Yang et al. (2006)	Water absorption test	Above 90% of the tensile strength
Yoon et al. (2007)	Chloride permeability test	Above 0.012 mm

2.8 CONCRETE BEHAVIOR UNDER ELEVATED TEMPERATURE

Although concrete is mostly subjected to the normal ranges of environmental temperature, there are some important conditions in which concrete is exposed to severe temperature changes such as fire, jet aircraft blast, furnaces and nuclear reactors. Therefore, understanding the behaviour of concrete at high temperatures and investigating the influence it has on physical properties of concrete is essential in order for reliable design criteria (Philleo 1958).

Concrete is composed of different constituents with different mechanical and physical properties which will be directly affected by thermal attack. It is well understood that concrete will be weakened by heating. Upon exposure to temperatures above 105 °C, concrete becomes more brittle and its materials undergo multiple microstructural alterations which result in significant reduction of concrete stiffness and integrity. However, more knowledge is required to fill the gap in the area of quantitative assessment of thermally induced damage in concrete.

Concrete deterioration under the effect of elevated temperature is through different mechanisms: (Fu et al. 2004 and Choinsla et al. 2007).

- Rapid evaporation of water during intensive heating provides high steam pressure which leads to microcrack propagation as relief channels for gas flow. Concrete surface spalling is the result of microcrack accumulation.
- Dehydration-induced microcracks are formed in the cement paste at 100 °C due to the mismatch in thermal expansion coefficient between various hydration products (C-S-H gel, calcium hydroxide and ettringite).

- The incompatibility of the elastic modulus between aggregates and cement paste upon drying also generates radial and circumferential cracking through concrete as shown in Figure 2.17 (Hearn 1999).
- Altering the pore size distribution and increasing the total porosity are other reasons leading to the loss of strength in concrete exposed to temperatures above 300°C.

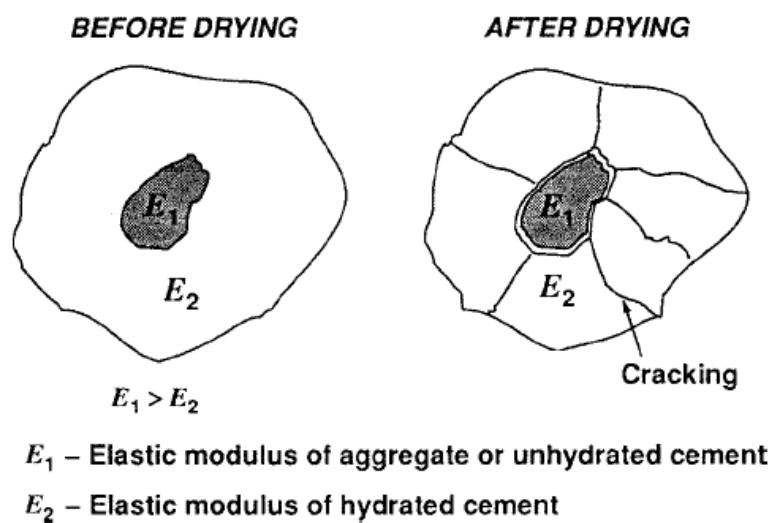


Figure 2.17 Drying shrinkage cracking (Hearn 1999)

In the experiment carried out by Figg (1973), the impact of microwave heating on compressive strength and modulus of elasticity of concrete was determined. A 5kW laboratory microwave and a 1.5kW commercial microwave oven were used as a source of energy. Concrete cubes were subjected to different heating duration. Results indicated a significant reduction in mechanical properties after 30 minutes microwave radiation. Compressive and tensile strength of concrete were decreased to 80% and 60% of the original value, respectively. Microwave drying also lowered the modulus of elasticity of specimens to 20% of the original value.

Samaha and Hover (1992) tested the permeability of concrete samples damaged either by compressive loading or drying shrinkage. As apparent from Figure 2.18, rapid chloride permeability of concrete was significantly increased when oven dried at 110°C. The average charge passed through oven dried specimens was 7 times more than air dried samples. They concluded that severe cracking caused by harsh drying has more destructive effect on concrete microstructure compared to the damage induced by one cycle loading.

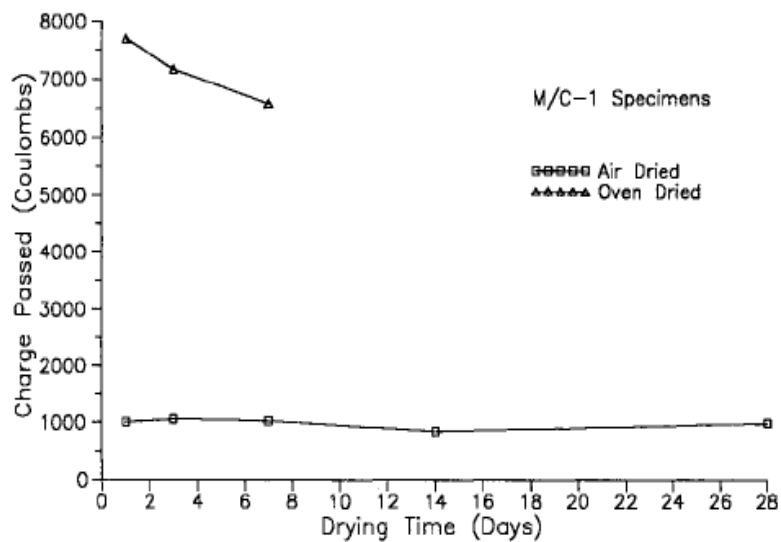


Figure 2.18 Effect of drying on total charge passed (Samaha and Hover 1992)

Kristensen and Hansen (1994) investigated the damage induced by thermal shock in cement paste and concrete specimens. To identify the presence of internal cracking due to rapid heating, ultrasonic pulse velocity was used. A significant increase in pulse transmission time was noticed for concrete cylinders instantaneously heated to a temperature above 50°C.

Martys and Ferraris (1997) compared the capillary water absorption of mortar samples oven dried at 50°C for the period of 20 days, with the air dried specimens at laboratory temperature. As illustrated in Figure 2.19, sorptivity for oven dried specimens is almost three times greater.

Shrinkage cracking results from oven drying process is the reason for a sharp increase in the amount of water uptake through mortars.

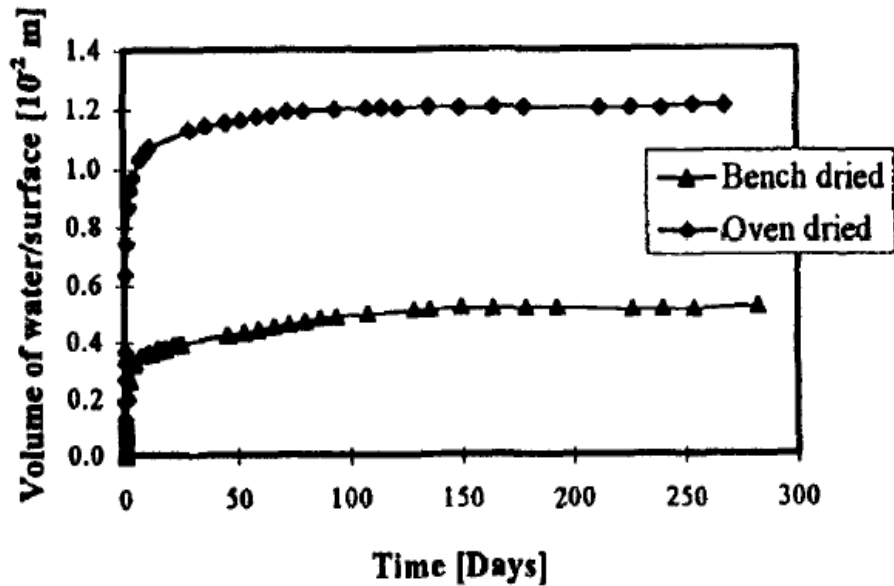


Figure 2.19 The influence of drying treatment on water absorption (Martys and Ferraris 1997)

The effect of drying shrinkage cracking on water permeability of concrete has been studied by Hearn (1999) in which concrete samples were subjected to rapid heating at 105°C before being loaded in different compressive stress levels. Results indicated that water permeability is not influenced by local damages result from short term loading up to 80% of the peak strength. However, uniform distribution of microcracks and joining of pores and internal flaws due to the oven drying seems to increase the water flow through concrete within one order of magnitude. On the other hand, shrinkage cracking results from oven drying caused the average decrease of 10% in ultrasonic pulse velocity. The coefficient of water permeability of concrete samples after being dried in the oven is shown versus the permeability of specimens in the virgin state for five different mixes in Figure 2.20.

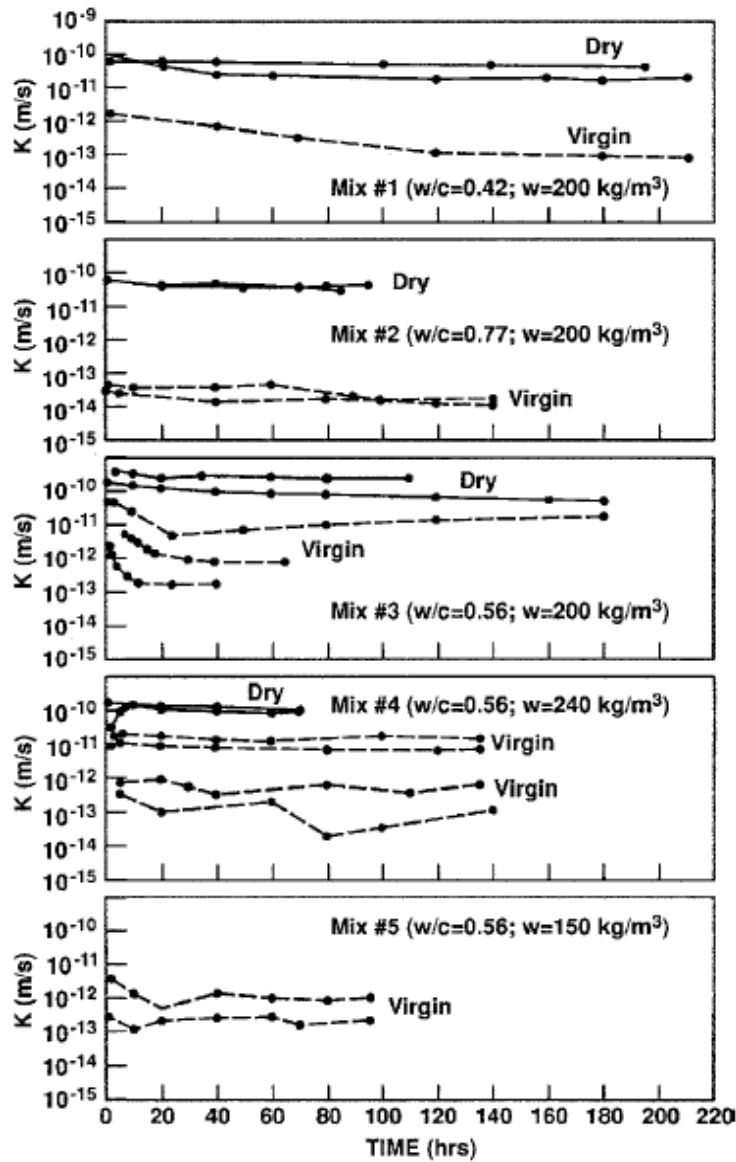


Figure 2.20 Coefficient of permeability versus time (Hearn 1999)

A recent study performed by Choinska et al. (2007), investigated the effect of damage induced by the combination of mechanical loading and high temperature on permeability of concrete. Hollow concrete cylinders were oven dried at 20, 105 and 150°C followed by compressive stress loading ranged from 20% to 90% of the peak stress. Each stress level was kept for 30 minutes to measure the gas permeability of concrete under loading. They found that although permeability was insensitive to stress levels below 80% of maximum load, application of high temperature resulted

in great permeability changes (Figure 2.21). Generally, an increase could be observed in gas permeability by increasing the temperature which would be due to the effect of pore widening and thermal induced microcracks.

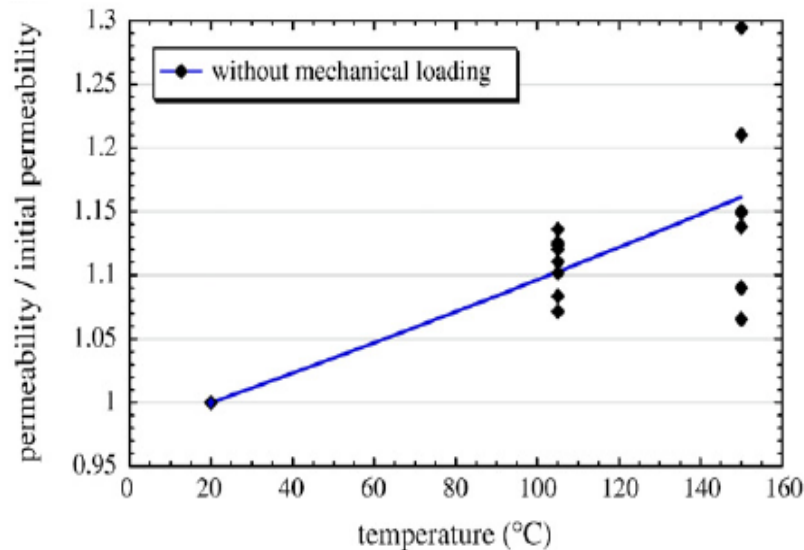


Figure 2.21 The effect of temperature on permeability without mechanical loading (Choinska et al. 2007)

2.9 THE EFFECT OF CONSOLIDATION ON CONCRETE PROPERTIES

The importance of construction practices on concrete performance has been well established qualitatively. However, the quantitative evaluation of construction defects and their influence on durability of concrete is of more interest. Permeability, resistance and surface appearance of concrete structures closely depend on the degree of consolidation. Consolidation is the process of compacting particles of freshly mixed concrete in order to remove the large pockets of entrapped air and provide more homogenous and dense concrete (Rasheeduzzafar et al. 1989 and ACI 309R-05).

Internal and external vibration are the most predominant ways for concrete consolidation. Vibration involves rapid motion of mixture ingredients which increase the fluidity of concrete by reducing the internal friction.

As air bubbles are expelled to the surface of the concrete, spaces around embedded steel reinforcement and the edges and corners of the formworks are filled by cement paste thus increasing the strength and uniformity of concrete (ACI 309.2R-98).

The most common factors leading to under-vibration are inappropriate selection of the type and number of vibrators, size, frequency and amplitude of vibration, shallow vibrator penetration, widely spaced insertion and insufficient insertion time. Serious deteriorations as a result of poor consolidation could be observed in the form of honeycombing, bug holes and irregular surface with excessive voids and cavities. As indicated by Whiting et al. (1987), each 5 percent increase in the amount of air content leads to 30% decrease in compressive strength of concrete.

On the other hand, over-vibration can also occur when the vibrating period exceeds the recommended time required for full vibration. Over-vibration leads to several imperfections such as formwork movement, sand streaking, aggregate transparency, bleeding and segregation (ACI 309.2R-98).

Bleeding is the upward displacement of water towards the surface of the concrete as a result of segregation and settlement of the solid particles. Bleed water is formed at the surface of the concrete in the plastic state, when the rate of bleeding exceeds the rate of water evaporation. Accumulation of bleed water makes the top surface of concrete porous and weakens the bond strength between concrete and reinforcement. High porosity of the concrete surface layer has a significant influence on permeability and mass transport properties of concrete and consequent

reduction of concrete durability. The higher the rate of bleeding the more the risk of plastic shrinkage cracking. Greater rate of bleeding could be observed in high slump concretes, badly proportioned mixtures and poor graded aggregates (Singh 2013 and Yim et al. 2013)

ASTM C 232 provides two test methods for measuring the amount of water bleeding from the surface of fresh concrete. Method A is for samples vibrated by rodding without intermittent vibration after being placed. While in the second method (method B), samples are subjected to intermittent periods of vibration (ASTM C232-09). Although the importance of consolidation has been clearly indicated, little information exists about the effect of insufficient compaction on concrete properties. Kaplan (1960) determined the influence of insufficient consolidation on compressive and flexural strength, dynamic modulus of elasticity and ultrasonic pulse velocity of concrete beams and cubes. Different void contents were obtained using different vibrating times with the maximum air void of 32 % in the samples placed without any compaction. Results showed a significant reduction in the concrete properties by increasing the void percentage regardless of the mix proportion and concrete age. Also it was proved that compressive strength is the most sensitive parameter regarding the incomplete consolidation. As can be seen in Figure 2.22, only 5% void content results in 30% and 24% decrease in compressive and flexural strength and only 2% reduction in pulse velocity.

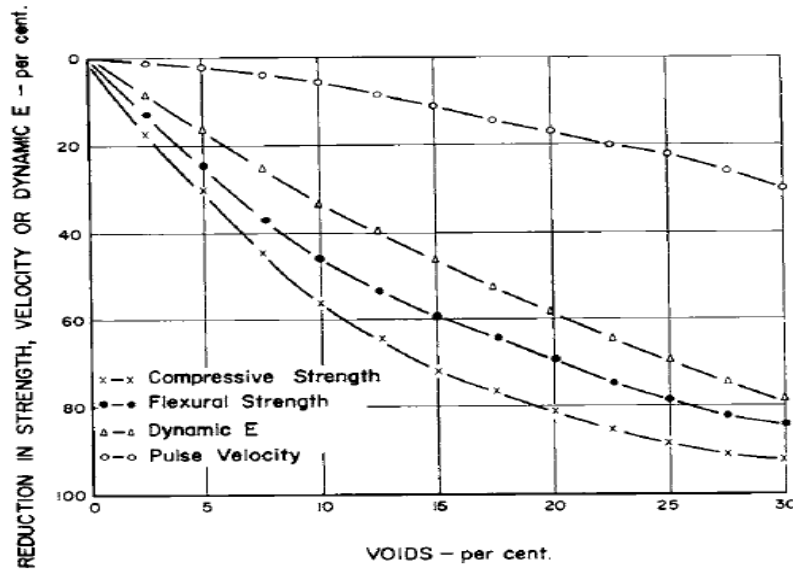


Figure 2.22 Different void contents versus concrete properties (Kaplan 1960)

Collepari et al. (1972) found that the coefficient of chloride diffusion for non-vibrated concrete specimens is almost twice as much as that of fully vibrated concretes. Another study by Whiting et al. (1987) investigated the effect of different degrees of consolidation including 100%, 92% and 85% on the most important properties of concrete with different mixtures. They found that inadequate level of consolidation results in a considerable decrease in compressive strength, chloride permeability resistance and bond strength between steel reinforcement and concrete while there was no significant change on freeze and thaw resistance. Compressive strength was reduced by 30% for every 5% decrease in compaction which is similar to the results obtained by Kaplan (1960). On the other hand, it was observed that over-consolidating to the primary level of segregation will improve the chloride resistance and strength characteristic of concrete as a result of entrapped air expulsion. Results can be shown in Figures 2.23 and 2.24.

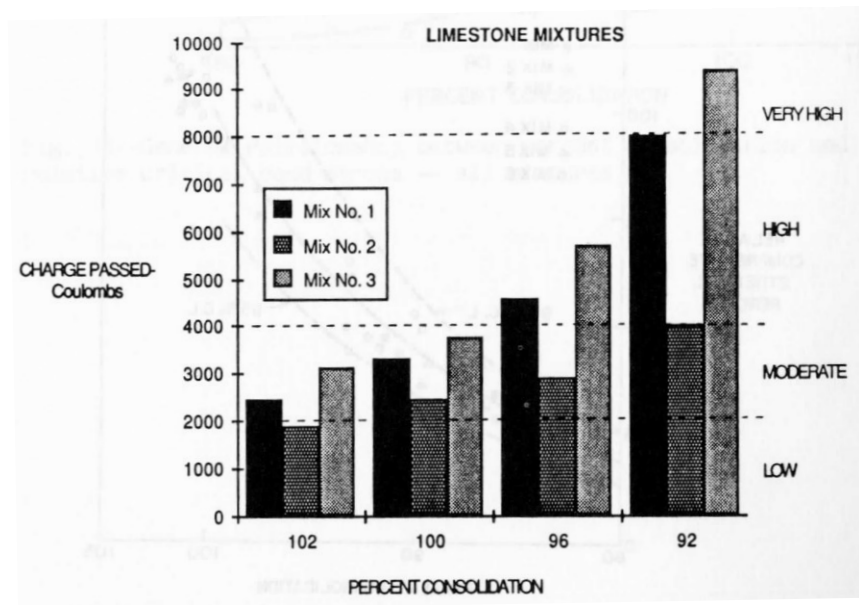


Figure 2.23 Relation between the charge passed and degree of consolidation (Whiting et al. 1987)

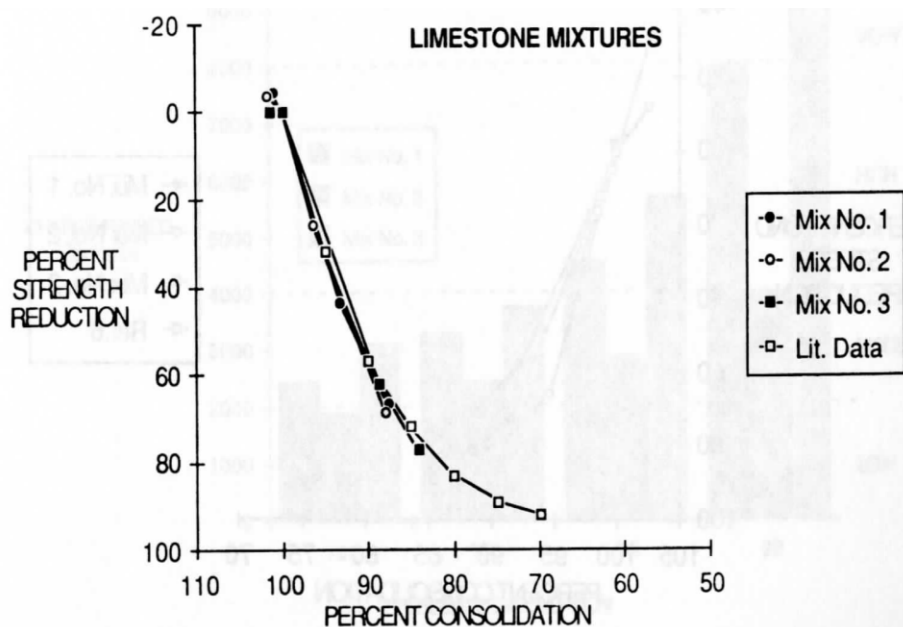


Figure 2.24 Relation between 28-day compressive strength and degree of consolidation (Whiting et al. 1987)

Research conducted by Rasheeduzzafar et al. (1989) on the effect of incomplete consolidation on reinforcement corrosion considering 30, 40, 60 and 80% degree of consolidation based on the time required to achieve full consolidation. Results indicated a significant decrease in the time of corrosion initiation as well as a noticeable increase in sulphate deterioration by decreasing the percentage of consolidation.

Popovics et al. (1990) investigated the influence of internal segregation on the ultrasonic pulse velocity of concretes and pastes. Velocity measurements at the top, middle and the bottom part of the specimens are shown in Figure 2.25. Although UPV of the paste specimens is independent of the location, concrete samples have much lower velocities at the top part of the concrete height.

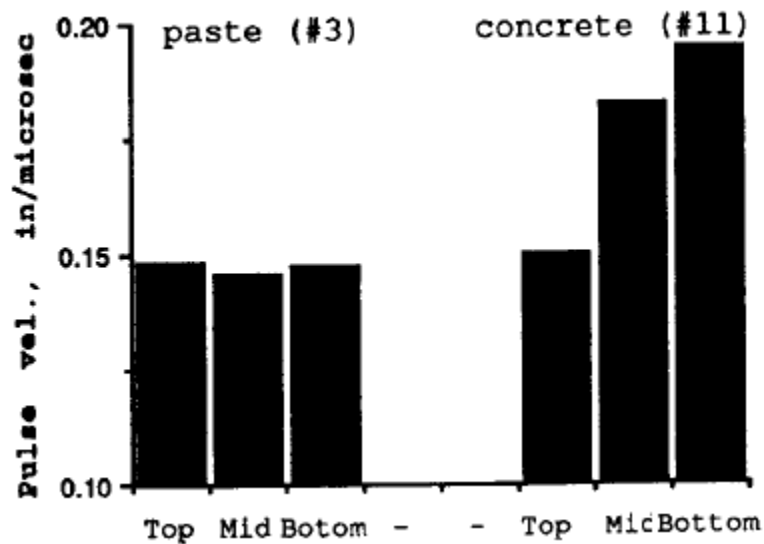


Figure 2.25 Location effect on the UPV of concrete and paste (Popovics et al. 1990)

The influence of insufficient consolidation on concrete durability was further emphasized by evaluating the chloride penetration of conventional and high strength concretes as a function of different levels of consolidation (Al-khaja 1997). It was shown that by decreasing the degree of consolidation from 100% (full consolidation) to 50% (incomplete consolidation), the chloride

content will be higher by 1.16 times and 1.23 times for conventional and high strength concrete, respectively.

In the work by Aldea et al. (1999), concrete discs cut from bottom, middle and top parts of the 100x200 mm cylinders were cracked to various extents and then subjected to rapid chloride permeability test in order to find the effect of segregation on electrical current. It was noticed that the location effect on total charge passed through concrete is variable at different crack widths (Figure 2.26).

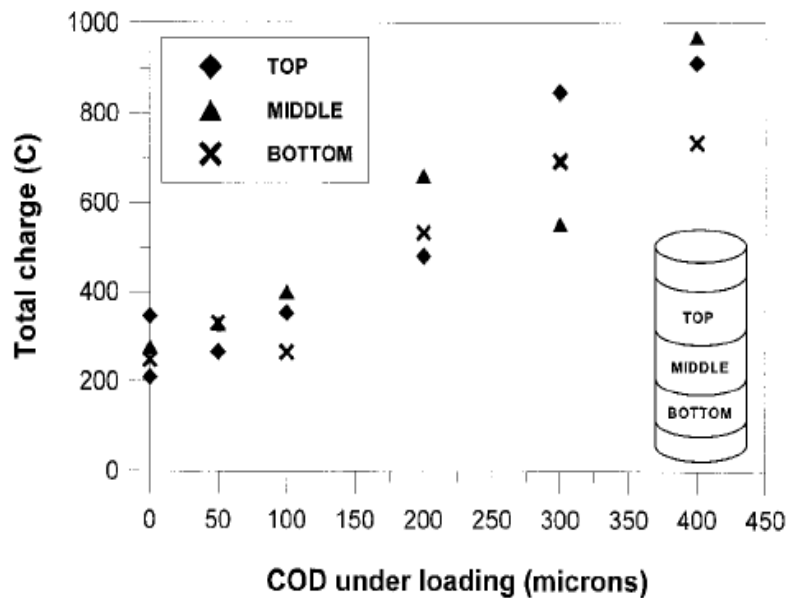


Figure 2.26 Location effect on chloride permeability of concrete (Aldea et al. 1999)

2.10 RESEARCH MOTIVATION

Performance specifications require evaluation of explicit characteristics that can be measured quantitatively. One of the considerable issues in this process is determining the point of performance; when and where properties are measured. Conventional “end of delivery chute tests” do not necessarily reflect placed concrete. Durability measurements based on the specimens in

well compacted, well cured and uncracked state provides an optimistic evaluation of concrete performance which is not an accurate representative of concrete behavior in real structures.

Construction defects such as improper consolidation is responsible for a significant amount of premature concrete deterioration (Mehta and Burrows 2001, Yang 2004). Despite the existing qualitative data, an attempt was made in this research to quantitatively assess the effect of wrong construction practices including over-vibration and insufficient consolidation on concrete performance and durability properties. This study will allow useful information for development of quality control specifications.

Cracking from either mechanical loading or thermal loading is another destructive defect that accounts for the rapid deterioration of concrete structures. Although different permeability test methods have been used in the literature to determine the effect of microcracks on water permeability of concrete, no standardized specification exists for measuring the water permeability. Therefore, the results of the permeability coefficient obtained using various approaches are not comparable. In contrast, there are specific standard test methods for concrete water absorption measurements. ASTM C 1585 is a simple standard test method assigned for measuring the rate of water absorption which can be used as an indication of concrete durability (Basheer et al. 2001). However, very little information exists on microcracks-water absorption relationship. As well, electrical conductivity test is a faster method compared with the time-consuming chloride permeability test (ASTM C1202) commonly used in the previous research.

Therefore, this study is intended to compare the effect of load-induced cracking, thermally-induced cracking and consolidation on concrete durability based on water absorption (ASTM C1585) and electrical conductivity (ASTM C1760) tests to find out how the existence of microcracking

modifies the mass transfer properties of concrete and accelerates the rate of deterioration. Table 2.2 shows the comparison between this study and previous work.

Table 2.2 Differences between this study and the previous research

Previous research	Current study
<ul style="list-style-type: none"> • Compressive loading • Covers limited stress levels 	<ul style="list-style-type: none"> • Tensile loading • Covers more stress levels
<ul style="list-style-type: none"> • Water permeability test <ul style="list-style-type: none"> - No standard method - Specific test device 	<ul style="list-style-type: none"> • Water absorption test <ul style="list-style-type: none"> - Standard method - Simple - Cost effective
<ul style="list-style-type: none"> • Chloride permeability test (ASTM C 1202) <p style="text-align: center;">Time: 6 hours</p>	<ul style="list-style-type: none"> • Electrical conductivity test (ASTM C 1760) <p style="text-align: center;">Time: 5 minutes</p>

3 EXPERIMENTAL PROGRAM

3.1 GENERAL DESCRIPTION

The experimental methodology for making and testing of concrete samples in the laboratory is described in this chapter. Generally, this research was intended to evaluate the effect of common construction defects on permeability of concrete which consists of three main phases:

1. Load-induced cracking

In this section, the influence of damage induced by mechanical loading on mass transport properties of concrete was studied. The type of loading was intended to produce a major crack through the sample. Concrete specimens were subjected to split tensile loading. After reaching to desired stress levels, samples were unloaded and examined by ultrasonic pulse velocity to identify the extent of cracking. The rate of water absorption and bulk electrical conductivity of damaged concretes were then measured according to the standard test methods ASTM C1585 and ASTM C 1760, respectively.

2. Thermally-induced cracking

The effect of drying shrinkage cracking resulting from elevated temperature on concrete durability was investigated in the second series of the tests. This loading was intended to produce a distributed network of cracking in the samples. A microwave oven was used for rapid heating of the specimens at different time durations. UPV was measured before and after the heating procedure to correlate the presence of microcracking with the changes in concrete behavior. Water absorption and electrical conductivity of the samples were also measured.

3. Inadequate vibration and over vibration

In order to show the importance of consolidation as a construction practice on the quality of finished concrete, one group of samples were fully vibrated according to the ASTM C 192 procedure. Another group of samples were cast without any vibration effort and the last group were purposely over vibrated until the appearance of bleeding and segregation. The effect of improper consolidation on the compressive strength of concrete was determined first. Samples were then tested for UPV, water absorption and bulk electrical resistivity.

The detailed information regarding the material and mixture proportions, sample geometry, equipment and test procedures is described as follows:

3.2 MATERIALS

The cement used in this work was ordinary Portland cement supplied by Holcim (Montreal, Canada) without any supplementary cementitious material. The coarse aggregate was crushed stone with the maximum size of 14 mm and a natural sand with the fineness modulus of 2.39 was used as fine aggregate.

Two concrete mixtures differing in the value of water-cement ratio were designed. The water to cement ratios selected represent the range typically used for concrete exposed to outdoor conditions in Canada. The concrete was air entrained and contained sufficient amount of water reducer to provide good workability. Mixture proportions are presented in Table 3.1.

Table 3.1 Concrete mixture proportions

Ingredient	Batch proportioning	
	Water/cement ratio	0.40
Water (kg/m ³ concrete)	187	187
Sand (kg/m ³ concrete)	624	688
Cement (kg/m ³ concrete)	433	346
Crushed stone 5-14 mm (kg/m ³ concrete)	941	941
Water reducer (mL/kg cement)	0-11.7	0-11.7
Air entrainer (mL/kg cement)	0.5	0.5

Water reducer dosage varied in different phases. Phase 1 and 2 contain 2.5 ml/kg cement of water reducer. The same amount of water reducer was used for the fully vibrated concrete in phase 3. But for the over consolidated samples the dosage was increased to 11.7 ml/kg cement. To avoid the effect of self-consolidation in high workability concrete, unconsolidated samples were mixed without using the water reducer admixture.

Concrete was cast in a pan-type mixer in the laboratory in accordance with the specifications of ASTM C 192. Unit weight, slump and air content of the freshly mixed concrete were also measured in accordance with ASTM C138, ASTM C 143 and ASTM C231, respectively.

For all three phases, the samples were demolded one day after casting and stored under lime-water at room temperature (23°C) prior to the time of testing (Figure 3.1). At the age of 56 days, compressive strength of hardened concrete was measured as per ASTM C39 by crushing three 100x200mm cylinders which were mixed and cured identically.



Figure 3.1 Samples in the curing bath

3.3 SPECIMEN DETAILS

3.3.1 Phases 1 and 2

In the first two parts of this study, 84 concrete cylinders with 100 mm diameter and 50 mm thickness were produced. The sample dimension was selected in order to meet the requirements of water absorption test. Sixty samples were tested for the effect of mechanical loading and the remaining samples were used for the thermal loading tests in the second phase. The specimens were fully consolidated in one layer by 25 rodding strokes as suggested in ASTM C 192.

3.3.2 Phases 3

Forty more concrete samples were cast to be used in the third section of this project. In order to better represent the effect of aggregate segregation through the depth of the concrete specimen, 200mm- height cylinders were used.

The first set of the specimens were fully consolidated in two layers by 25 rodding strokes as suggested in ASTM C 192. But for the next group of samples, concrete was simply poured in to the molds without being compacted and the top surface was leveled with the minimum amount of troweling. This leads to the finished concrete with an excessive amount of entrapped air. The void content of unconsolidated samples was measured as a percentage of the average weights of the fully vibrated specimens. This void content is in addition to the air entrained admixture intentionally mixed with concrete to improve its freeze and thaw resistance. Figure 3.2 shows the appearance of non-vibrated samples compared with the fully vibrated one. A non-uniform distribution of air voids through concrete volume can be observed with irregular shapes and sizes.



Figure 3.2 Surface appearance of unconsolidated sample (left) versus full compacted sample (right)

In the final test series, samples were over consolidated using a vibrating table with the frequency of 60 Hz. Vibration was allowed for the period of 10 minutes to ensure the appearance of bleed water at the surface of the concrete. For each mixture, three extra samples were cast to measure

the quantity of bleed water. The test procedure was according to the method A described in ASTM C 232 except the size of the container. A cylindrical mold with 100 mm diameter and 200mm height was used to measure the bleeding rate.

After being vibrated, concrete top surface was smoothed and the mass of the mold containing the concrete sample was measured. Samples were then cap covered and left on the vibration free floor in the ambient temperature of the laboratory for the period of 40 minutes. Free water accumulated on the top surface of the specimen was withdrawn by means of a pipet and it was collected in the small metal beaker. The beaker was put inside the oven at 110 °C for 24 hours to remove the mass of the sludge and other impurities. The amount of bleed water was calculated as follows: (ASTM C232-09)

$$V = \frac{V_1}{A} \quad \text{[Equation. 3.1]}$$

where:

V_1 = Volume of bleed water (mL)

A= Exposed surface area of the concrete (cm²)

Before starting the test procedure at the age of two months, concrete discs of 50 mm thickness were extracted from the middle part of the fully vibrated and non-vibrated cylinders using a masonry saw. But to better observe the effect of segregation, over vibrated samples were sawn from two different locations. One disc was cut from the top part of the cylinder which mostly contains the cement paste and another disc was cut from the bottom end of the cylinder with more aggregate in it.

3.4 TESTING PROCEDURES

3.4.1 Splitting tensile test

Tensile strength of concrete can be determined by three main methods: direct tension, modulus of rupture (flexural) test and splitting test (Lin and Wood 2003). The sample holding device for the direct tension test method induces secondary stresses that cannot be ignored and is difficult to carry out. The flexural tests are carried out on beams and produce cracking on only the tensile side of the specimen. The type of cracking as well as the added difficulty in obtaining samples of the correct dimensions makes it less than ideal. The splitting tensile test, also known as the Brazilian test, is an indirect measurement of concrete tensile strength which was first proposed by Carneiro and Barcellos in Brazil in 1953 (Lin and Wood 2003). Later it was established as a standard test method in which a diametrical compressive force is applied along the length of the specimen until failure occurs in the vertical plane.

Splitting tensile strength (T) in MPa can be calculated using the following equation (ASTM C496-11):

$$T = \frac{2P}{\pi ld} \quad \text{[Equation. 3.2]}$$

Where:

P= Maximum induced load at failure (N)

l= Specimen length (mm)

d= Specimen diameter (mm)

At the end of the curing period, concrete cylinders were cracked using the Brazilian splitting tensile test. As shown in Figure 3.3, concrete cylinders were placed horizontally between the surfaces of the loading platens in an 1100 kN capacity Forney compression testing machine. Two plywood

strips 3 mm thick and 25mm wide, were placed between the ends of the concrete sample and both upper and lower steel blocks to allow uniform load distribution and to avoid high stress concentration around the area of the loading points. All the specimens were loaded with the constant rate of 0.7 to 1.4 MPa per minute as indicated by ASTM C 496 until reaching the predetermined stress levels expressed as the percentage of the maximum tensile strength.

The ultimate tensile capacity of concrete (f_u) was calculated as the average crushing strength of three 100x50 mm cylinders, using Equation 3.2. The remaining specimens for this phase were tested at various percentages of the ultimate load. The target stress levels ranged from 20% to 90% of the peak tensile strength at equal intervals of 10%. Each stress level was kept for 10 minutes prior to unloading to allow crack propagation. Three specimens were produced at each load level.



Figure 3.3 Brazilian test setup

3.4.2 Microwave heating

Investigating the effect of thermal induced cracking on the mass transport properties of concrete was the purpose of the second part of this project. For this, three specimens from each mixture were first put inside the microwave oven in order to find the maximum heating time. Samples could sustain microwave irradiation for the average time of 5 minutes before exploding. Therefore, samples were heated for the duration of 1, 2 and 3 minutes using a 1.5 kW microwave oven. The surface temperature of the concrete samples was then measured by an infrared thermometer (Figure 3.4).

Since the extent of damage induced by microwave heating depends on the concrete degree of saturation, all the specimens were tested in the saturated surface dry condition which reflects the most severe deterioration.

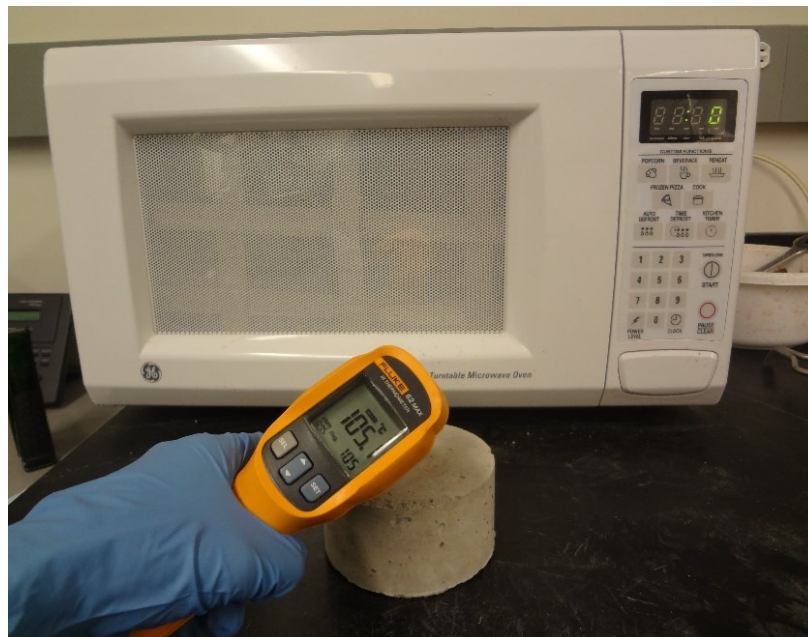


Figure 3.4 Temperature measurements after microwave heating

3.4.3 Ultrasonic pulse velocity

Ultrasonic pulse velocity was used as a non-destructive method of microcrack evaluation. The principle of this method is that the velocity of ultrasonic waves through concrete will be decreased by internal flaws and microcrack propagation (Malhotra and Carino 2004).

According to Jones (1952) and Raju (1970), cracking will occur parallel to the direction of loading in the cylinders compressed across their diameter. Thus, UPV remains constant in the axis of loading. In this study, pulse velocity was measured perpendicular to the loading direction before and after loading to quantify the extent of damage results from each stress level. Figure 3.5 illustrates the Proceq Pundit device used for the UPV test.



Figure 3.5 Ultrasonic pulse velocity test device

A portable ultrasonic unit consisting of two transducers as a pulse wave generator and a pulse receiver was used to measure the velocity of the longitudinal waves. Transducers were attached to the opposite sides of the specimen through an Aquasonic gel as a coupling agent to provide better

contact between transducers and the rough surface of the concrete. The time taken for traveling the pulse through concrete between the centres of the transducers was measured and displayed in tenths of microsecond. Subsequently, velocity was calculated by dividing the path length (L) over the transmission time (T) as follows (Malhotra and Carino 2004):

$$v = \frac{L}{T} \quad \text{[Equation. 3.3]}$$

In a dispersive material such as concrete, the velocity of a vibration pulse will be affected by the pulse frequency. Therefore, care must be taken to use the suitable frequency depending on the sample dimension and geometry (Popovics et al. 1990). According to the ASTM C597, frequency is selected in order to provide the pulse wavelength greater than the maximum size of coarse aggregate and smaller than the minimum size of the test specimen.

In this study, measurements were made with 150 kHz frequency. As stated by Wu and Wang (2000), the longitudinal wave velocity in normal strength concrete is in the range of 3000 to 5500 m/s. With the maximum size of 14 mm for coarse aggregates and the minimum sample dimension of 50 mm, frequency was calculated based on the Equation 3.4.

$$v = f \lambda \quad \text{[Equation. 3.4]}$$

where:

v: Pulse velocity (m/s)

f: Frequency (Hz)

λ : wavelength (m)

Moisture content of concrete sample is another factor affecting the ultrasound pulse velocity (ASTM C597-09). Thus, all the measurements were made in the saturated surface dry condition.

For this aim, a damp paper towel was used to dry the surface of the saturated samples before UPV measurements.

3.4.4 Water absorption

As mentioned before, sorptivity is the capillary rise of water molecules through an unsaturated permeable material in the absence of external pressure. Sorptivity is determined by measuring the rate of water absorbed through concrete surface during a specific period of time.

The test procedure used for measuring the rate of water absorption followed the steps indicated by ASTM C 1585. Concrete discs of 100 ± 6 mm diameter and 50 ± 3 mm thickness were preconditioned in an environmental chamber with a relative humidity of $80 \pm 3\%$ and temperature of $50 \pm 2^\circ\text{C}$ for 3 days (Figure 3.6). Then they were separately stored in the sealed plastic bags for the period of 15 days at the room temperature of $23 \pm 2^\circ\text{C}$ to allow moisture equilibration throughout the concrete depth.

The curved side of the specimens were sealed using a vinyl electrical tape and only the bottom surface of the samples was in contact with water to ensure one dimensional flow rate. The top side of the concrete samples were covered with a plastic sheet to avoid moisture evaporation during the test.

Then, the samples were placed on the supports inside the shallow container filled with tap water to the depth of 1-3 mm above the support surface. The water level was kept constant during the test. Samples were removed from the pan and the mass was determined with an accuracy of 0.01 grams. Water absorption measurements were made at the temperature of 23°C . The schematic of test procedure is depicted in Figure 3.7.

Initial sorptivity was measured by recording the incremental mass changes of concrete specimens at regular time intervals during the first 6 hours. Measurements were continued once a day for the next 8 days to obtain the secondary sorptivity. All the calculations were made based on the Equations 2.1 and 2.2.

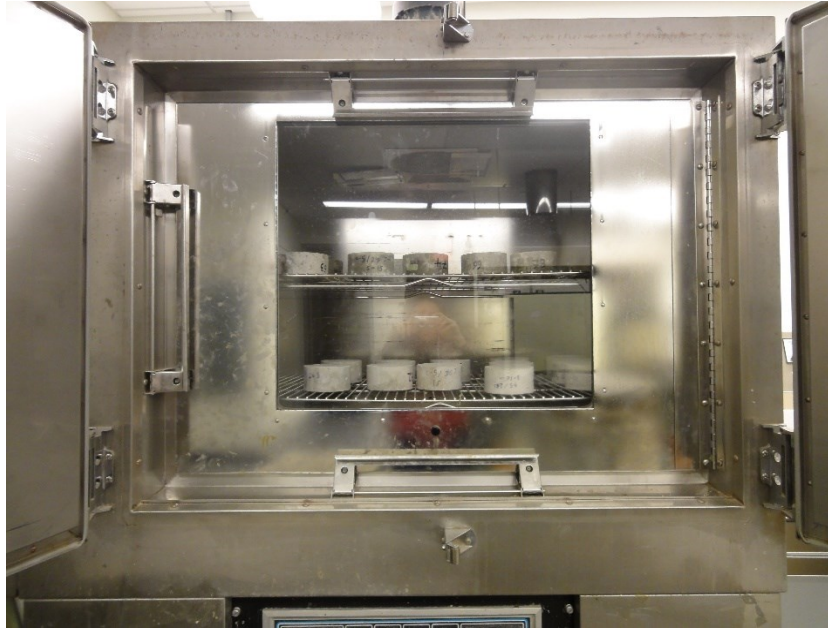


Figure 3.6 Samples in an environmental chamber

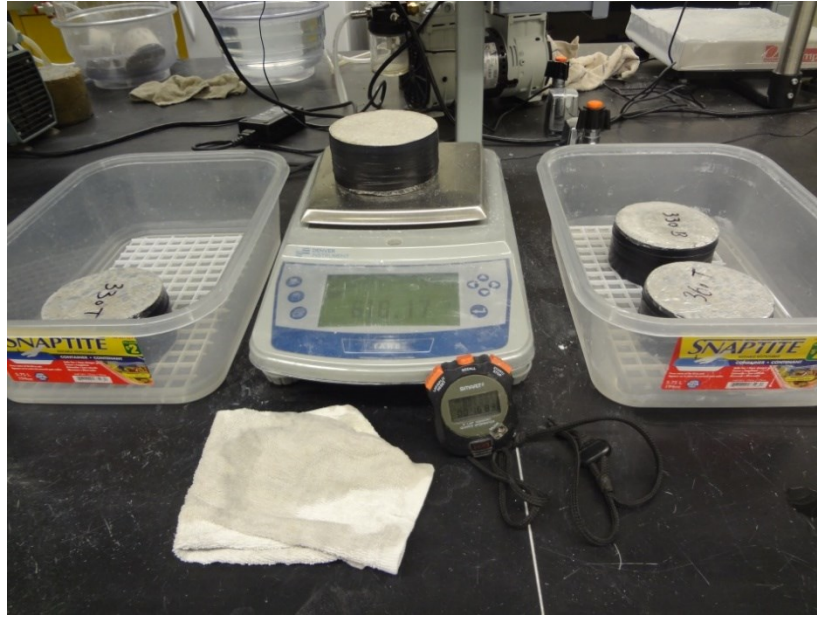


Figure 3.7 Water absorption test setup

3.4.5 Bulk electrical conductivity

Several test methods have been developed to assess the chloride permeability of hardened concrete as an important factor influencing the durability and performance of concrete structures. Bulk electrical conductivity can be used as a rapid indication of concrete resistivity against chloride penetration which is measured in accordance with the ASTM C 1760. This method is based on accelerating the chloride ion migration through saturated concrete sample under the force of an external electrical field (Samaha and Hover 1992, Basheer et al. 2001 and Sillanpaa 2010). The increasing interest in measuring the electrical properties of concrete as a quality control tool is due to the simple, cost effective and very short time test procedure (Spragg et al. 2013).

In the bulk electrical conductivity test, chloride ions are forced to pass through a concrete sample of 50 mm thickness and 100 mm diameter and the amount of electrical charge is measured under the potential differences of 60 V. The higher the electrical conductivity indicates the greater the concrete permeability.

The test procedure began with sample conditioning as explained by ASTM C 1202. Specimens were put inside the vacuum desiccator for 3 hours. De-aired water was then added to the desiccator to fully cover the samples. Vacuum saturation was continued for one additional hour before releasing the vacuum pump. Air was allowed to enter the system and samples were immersed under the water for 18 hours prior to performing the test (Figure 3.8). Subsequently, sample was clamped between two halves of the test cell which were filled with 3% sodium chloride solution. Care must be taken to provide adequate sealing between concrete and the cells to avoid leakage. The voltage cell was connected to the main power supply in order to apply the direct voltage of 60 V across the ends of the specimen. The time and total amount of current passed through concrete was recorded and displayed in the computer program. The test was performed using the German PROOVE'it rapid chloride permeability test apparatus as shown in Figure 3.9.

The bulk electrical conductivity was calculated based on the following equation (ASTM C1760-12):

$$\sigma = k \frac{I_1}{V} \frac{L}{D^2} \quad \text{[Equation. 3.5]}$$

where:

σ : Electrical conductivity (mS/m)

I_1 : Current at 1 min (mA)

V: Voltage (Volt)

L: Specimen length (mm)

D: specimen diameter (mm)

k: conversion factor= 1273.2

Due to the measurement recording limitations of the equipment, the current was recorded at 5 minutes. But as no heating occurs during this short time frame, it is not expected to be different than that measured at one minute.

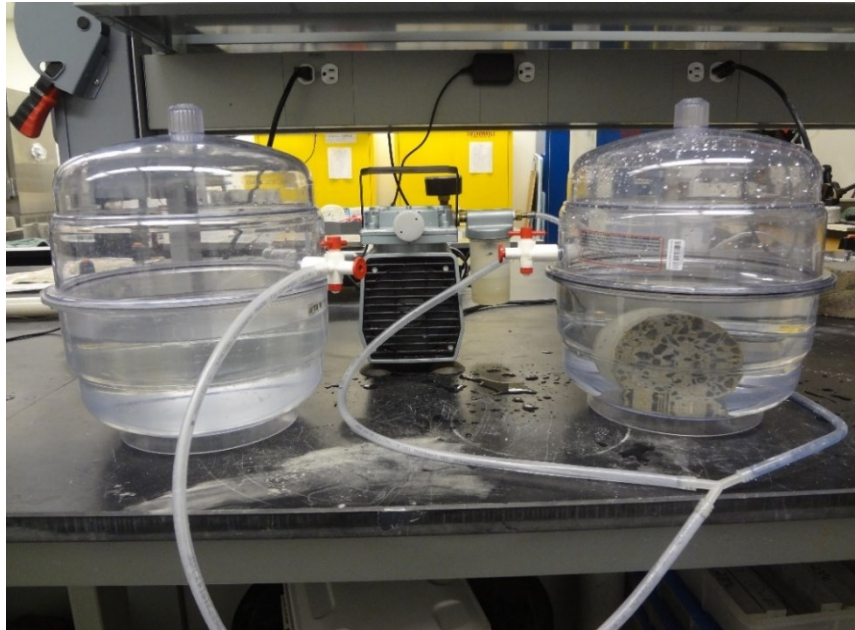


Figure 3.8 Vacuum saturation device



Figure 3.9 Bulk electrical conductivity test set up

Measuring the electrical conductivity for the unconsolidated specimens was not possible. The high volume of interconnected air voids inside the concrete specimen makes a short circuit which allows the sodium chloride solution easily passing through the concrete sample prior to the voltage application. Therefore, electrical resistivity test was performed for these samples rather than the electrical conductivity test.

3.4.6 Bulk electrical resistivity

Electrical resistivity is a non-destructive test method which indicates the concrete resistance against electron transport process. Electrical properties of concrete can be used as an indirect assessment of the pore system characteristics and concrete microstructure which is linked to the mass transfer properties of concrete. The electrical resistivity measurements can also be used to estimate the risk of reinforcement corrosion due to the chloride penetration through concrete (Huang 2006 and Shahroodi 2010).

Electrical resistivity tests can be classified as surface resistivity test, also known as Wenner test, which is more suitable for the 100x200mm cylinders and the bulk electrical resistivity test. In this project, the bulk electrical resistivity of concrete was measured using a PROCEQ unit (Figure 3.10).

A saturated surface dry specimen was placed between two plate electrodes. Two wet foams were also put on the top and bottom ends of the specimen to provide better connection between the concrete surface and electrodes. An electrical circuit was made through the pore network of the concrete structure under a potential difference. Concrete resistivity was then measured based on the following equations (PROCEQ manual 2012):

$$\rho = K.R_{cylinder} \quad [\text{Equation. 3.6}]$$

$$R_{cylinder} = R_{measured} - R_{upper} - R_{lower} \quad [\text{Equation. 3.7}]$$

$$K = A/L \quad [\text{Equation. 3.8}]$$

In which:

ρ : Bulk resistivity (k Ω .cm)

$R_{measured}$: Resistance of the sample, top and bottom foam (k Ω .cm)

R_{upper} : Resistance of the top foam (k Ω .cm)

R_{lower} : Resistance of the bottom foam (k Ω .cm)

A: Surface area of the sample (cm²)

L: Sample length (cm)



Figure 3.10 PROCEQ unit used to measure the electrical resistivity

4 RESULTS AND DISCUSSION

4.1 INTRODUCTION

This chapter contains the test results obtained for the different phases. The results are analyzed and discussed with the relevant findings. Each result represents the average observation of three samples tested at the same condition. For the water absorption test, the variations among three measurements from the average value were mostly within 6 % as indicated by ASTM C 1585. Any differences greater than 8% were omitted from the results. Also, there were less than 10% differences in the measured electrical conductivity among three replicate specimens.

The properties of concrete measured at fresh and hardened states for all three phases are presented in Tables 4.1 and 4.2 (Details of these procedures can be found in Chapter 3). Generally, samples with the lower water to cement ratio have higher compressive and tensile strength corresponding to the greater density and lower workability. The slump is the highest in the over vibrated concrete due to the use of extra water reducer admixture. The minimum slump was obtained for the non-vibrated specimens in which water reducer was not added. The void content was calculated based on the differences in the weight of the fully vibrated and non-vibrated samples. As a result of self-consolidation, the void content in the higher w/c mixture is somewhat less than that of the w/c=0.4 mixture. Also, there is a significant decrease in the volume of bleed water in concrete with lower water-cement ratio since the contribution of mixing water in the hydration reaction will be increased by increasing the cement content (Wainwright 1955); whereas, more water is available for bleeding in the higher w/c concrete.

Table 4.1 Concrete properties measured for Phases 1 and 2

Phase 1 and 2					
W/C ratio	Air content (%)	Slump (mm)	Unit weight (kg/m ³)	Average compressive strength (MPa)	Average tensile strength (f _t) (MPa)
0.4	6.0	100	2384	44.3	4.36
0.5	6.0	150	2301	37.2	3.79

Table 4.2 Concrete properties for Phase 3

Phase 3						
W/C ratio	Degree of consolidation	Air content (%)	Slump (mm)	Unit weight (kg/m ³)	Bleeding (mL/cm ²)	Void content (%)
0.4	Full vibration	6.0	100	2405	-	-
	Over-vibration	6.0	150	-	0.006	-
	Non-vibration	6.0	70	-	-	17.8
0.5	Full vibration	6.0	150	2320	-	-
	Over-vibration	6.0	200	-	0.011	-
	Non-vibration	6.0	80	-	-	15.1

4.2 RESULTS FOR PHASE 1

4.2.1 The effect of load-induced cracking on ultrasonic pulse velocity

The relation between different levels of tensile loading and the average changes of the pulse velocity is depicted in Figure 4.1. Each point on the graph represents an average of three samples loaded to the same stress level. Although a gradual decrease in the UPV was expected by increasing the stress levels, UPV remained relatively constant between uncracked state and the load level up to about 70% of the peak strength. This is in agreement with the previous research indicating that UPV is unaffected by increasing the load level, to a large extent (Raju 1970, Shah and Chandra 1970, Hearn 1999, and Shokouhi and Niederleithinger 2012).

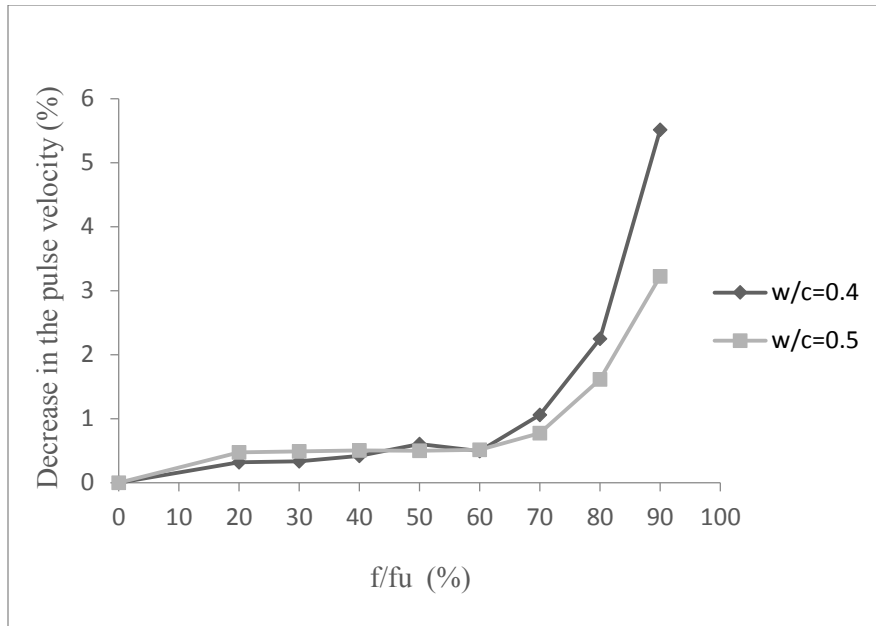


Figure 4.1 Effect of tensile loading on pulse velocity of concrete

Microcrack recovery due to the concrete's elasticity is a hypothetical explanation for the insensitivity of pulse velocity prior to the peak strength (Shah and Chandra 1970, Hearn 1999). Under microscopic examination; Lim et al. (2000) found that microcrack recovery is 100% for stresses below $0.5 f_u$ (Figure 4.2). Between $0.5-0.7f_u$, interfacial cracks around the aggregates tend to close back partially after complete unloading, thus reducing the crack opening displacement making it too small to be detected by the pulse wavelength. According to Yang (2004), only the presence of large visible cracks will have a noticeable effect on the UPV.

At higher load steps ($0.7-0.9f_u$), formation of mortar cracks and widening of existing cracks lead to the relatively sharp decrease in the pulse velocity by more than 5% and 3% for water to cement ratios of 0.4 and 0.5, respectively. The total decrease in pulse velocity in the former studies varied depending on the specimen geometry and pulse frequency.

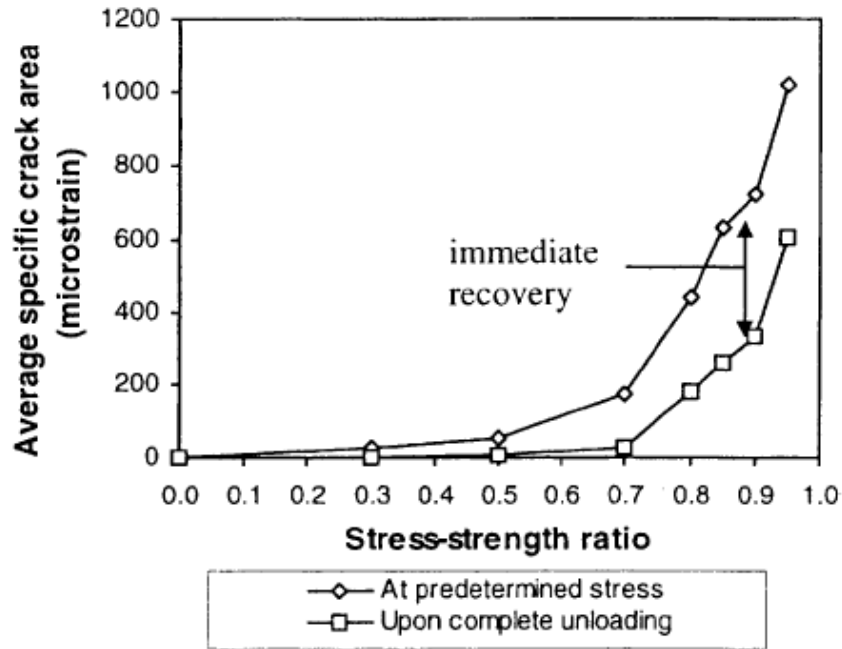


Figure 4.2 Microcrack recovery after unloading (Lim et al. 2000)

4.2.2 The effect of load-induced cracking on water absorption

The results of the water absorption test as a function of square root of the time for the intact specimens at 0% loading is presented in Figure 4.3. Each curve consists of two regions linearly relating the rate of water absorption to the square root of the time. Sorptivities were measured as the slope of the lines with the correlation coefficients (R^2) above 0.97. Data up to six hours (~ 147 s^{1/2}) were used to calculate initial sorptivity and later measurements up to 8 days determined the secondary sorptivity.

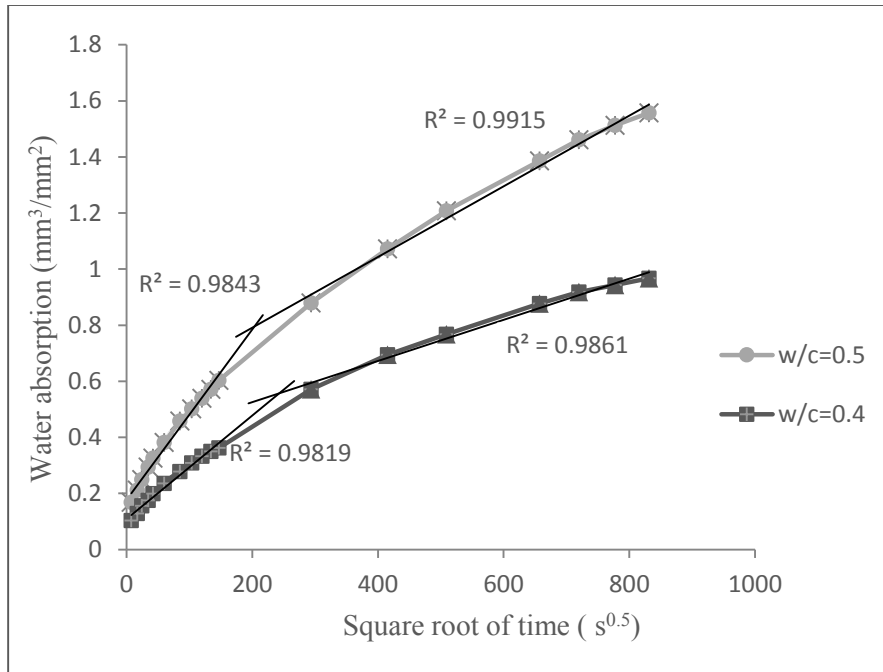


Figure 4.3 Water absorption results for specimens at stress-free state

An increase can be seen in the rate of water absorption with the faster rate for higher water to cement ratio. But after the initial hours of exposure, the rate of water movement through concrete decreased significantly due to the increase in the saturation degree of concrete and the consequent decrease in the capillary suction forces (Martys and Ferraris 1997 and Castro et al. 2011).

The effect of tensile induced cracking on the rate of water penetration through concrete can be summarized in Figures 4.4 and 4.5 which show the relationship between different stress levels and initial and secondary sorptivity, respectively. The individual results are also shown on the figures. It is clearly evident that samples with the higher water to cement ratio are more water permeable for the entire stress range due to the higher porosity and pore connectivity of the concrete in this mixture. In general, the values of initial sorptivity are greater than the secondary sorptivity at all stress levels.

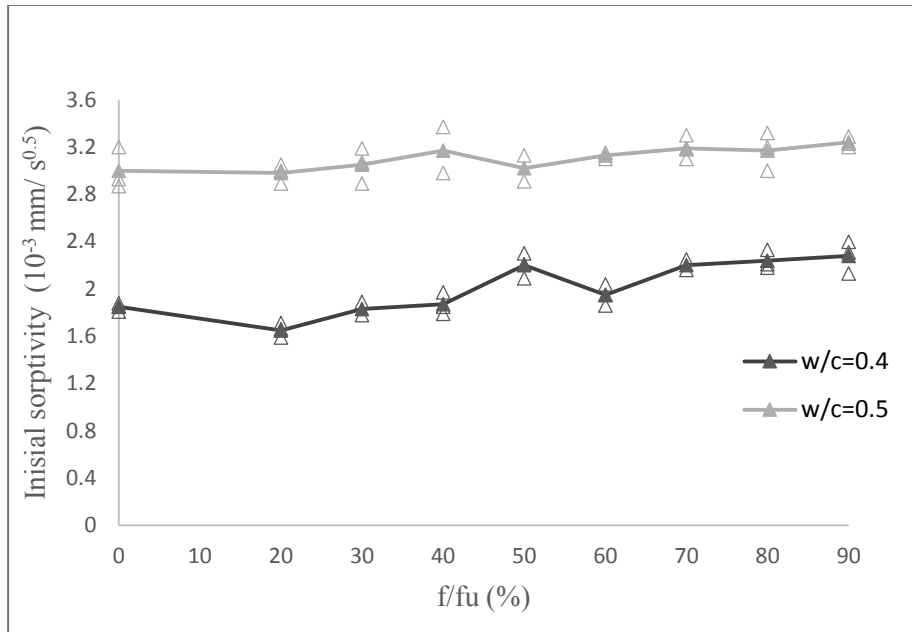


Figure 4.4 Initial water sorptivity versus stress-strength ratio

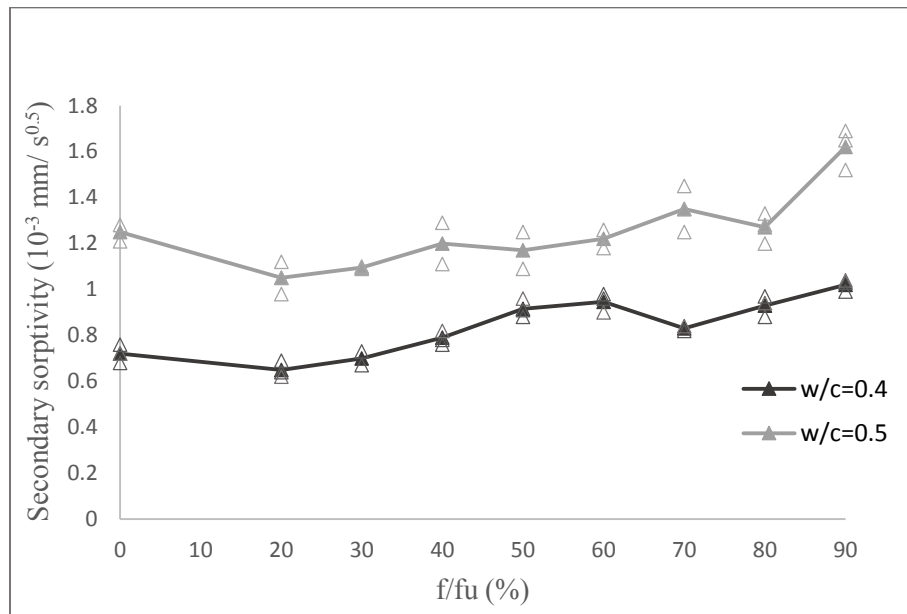


Figure 4.5 Secondary water sorptivity versus stress-strength ratio

While still there is a total tendency towards increasing the water absorption by increasing the degree of load-induced damage, concrete does not follow any direct pattern relating the water sorptivity to the percentage of applied load.

A slight decrease can be observed in the values of initial and secondary sorptivity under small loading between 0-20 percent of the maximum strength. This may be attributed to the effect of pore compression which leads to the closure of existing voids and microcracks and consequent reduction of concrete permeability at low stress levels (Raju 1970, Popovics et al. 1991, Yang 2004 and Bhargva and Banthia 2006).

For the initial sorptivity, a very small increase was generally observed with increase in stress-strength ratio. For $w/c=0.4$, initial sorptivity of concrete started from $0.00185 \text{ mm/s}^{0.5}$ at stress free state and reaching to $0.00228 \text{ mm/s}^{0.5}$ at $0.9f_u$. The maximum differences of 8% was achieved in the initial sorptivity of concrete with $w/c=0.5$, when loaded to 90% of the ultimate capacity.

However, the effect of load induced damage on secondary sorptivity of concrete is considerably more pronounced, especially when exceeding 80% of the loading capacity. Increasing the stress level from 0 to $0.9 f_u$, results in 41% and 30% increase in the secondary sorptivity of concrete with $w/c=0.4$ and $w/c=0.5$, respectively. For the secondary sorptivity, some variability in the results can be seen as well. This is consistent with the results presented by Hearn (1999) in regards to stress and water permeability. The insensitivity of water absorption in response to the tensile loading below $0.8f_u$ can be explained by the type, location and the extent of mechanically induced cracking. Previous research by microscopic examination revealed that bond cracking begins to form at the aggregate-paste interface at stress levels below $0.7f_u$ which are few in number, localized, and disconnected with partial recovery after unloading. The mass transport properties of concrete is only marginally affected by the formation of these localized, discrete cracking that predominantly

appears under low stress levels. The results of AE energy analysis performed by Yang et al. (2006) have proved the localized influence of damage results from tensile loading.

Whereas, beyond 70% of the ultimate strength ($0.7-0.9f_u$), mortar cracks are propagating noticeably through the cement matrix and bridging to the adjacent bond cracks thus creating a continuous crack network. The coalescence of interfacial and mortar cracking near failure provides interconnected pathways for water and liquid flow through concrete and increases its permeability (Smadi and Slate 1989, Samaha and Hover 1992, Saito and Ishimori 1994, Krishnaswamy 1969, Hearn 1999 and Yang et al. 2006).

4.2.3 The effect of load-induced cracking on electrical conductivity

The results of bulk electrical conductivity are plotted against the corresponding stress – strength ratio in Figure 4.6. The individual results are also shown on the figure. Some of the samples were omitted from the results due to the cell leakage. In these cases, electrical conductivity was measured as the average of two specimens. Although the higher w/c concrete is more conductive at all stress levels by at least 30%, a similar trend can be observed in response to the degree of cracking for both mixtures. While electrical conductivity increases in overall, there is a notable decrease in the 50% to 70% loading range. At first thought, this could be attributed to non-uniform behaviour among the three replicate samples, but the results were within 10% of the average at all stress levels. The reason for this reduction may be due to the effect of pore compression under the applied stresses below 70% of the peak strength. Again, similar variable behaviour was detected by other researchers at stress levels less than $0.7f_u$ (Samaha and Hover 1992, Saito and Ishimori 1994 and Aldea et al. 1999).

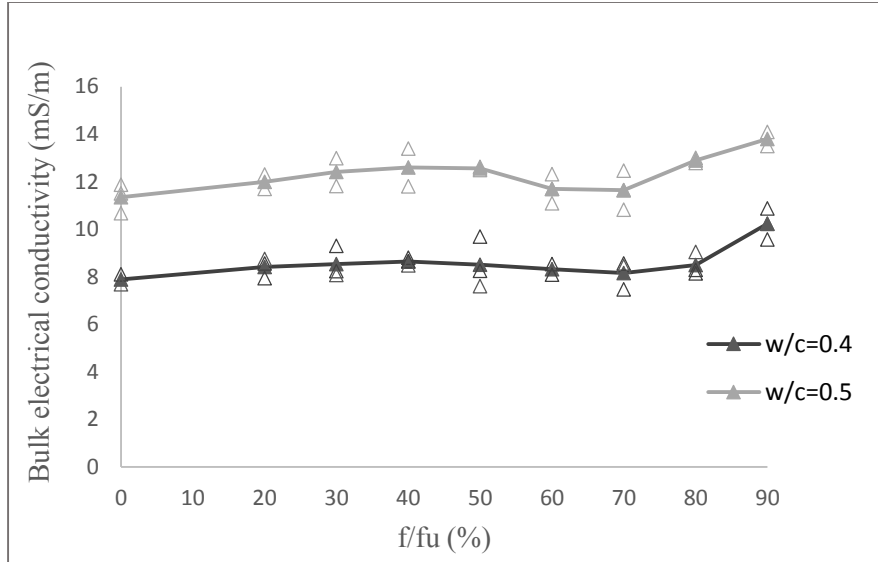


Figure 4.6 Bulk electrical conductivity versus stress-strength ratio

Figure 4.7 exhibits the amounts of electrical conductivity normalized to that of unloaded reference samples. Concrete conductivity is not significantly affected below 70% of the peak strength. As discussed earlier, this is due to the lack of well distributed crack pattern required to increase the concrete permeability. However, beyond $0.7f_u$ crack extension in to the mortar matrix is more likely to occur, thus increasing the overall porosity of the concrete. A change in the load level from 0% to 90% of the ultimate strength will coincide with about 30% increase in the concrete electrical conductivity for samples with the water to cement ratio of 0.4 and above 20% increase for $w/c=0.5$, suggesting a critical damage development in the system.

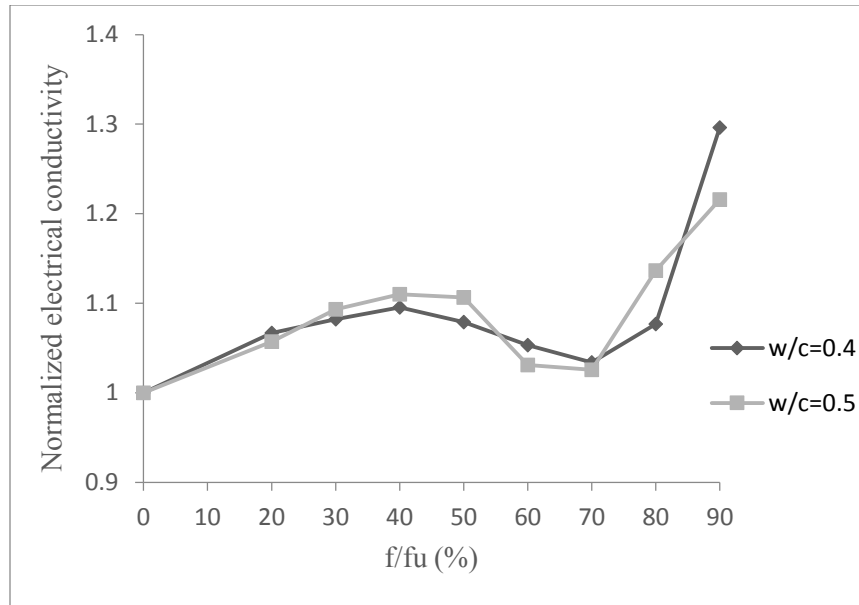


Figure 4.7 Normalized electrical conductivity versus stress-strength ratio

Although higher values of electrical conductivity were recorded for the samples with higher water to cement ratio, the effect of cracking on increasing the concrete conductivity is more highlighted in lower water to cement ratio at least for the range included in this study. This agrees well with the results obtained by Aldea et al. (1999) (refer to Figure 2.12)

4.3 RESULTS FOR PHASE 2

4.3.1 The effect of thermal induced cracking on ultrasonic pulse velocity

Tensile stress development due to the thermal expansion differences between the aggregates and cement matrix of instantaneously heated concrete will generate microcracking which may not be visible on the specimen surface. Therefore, the ultrasonic pulse velocity technique was applied to identify the presence of internal damage resulting from thermal shock. UPV was measured once concrete specimens were removed from the curing bath. Samples were then subjected to rapid drying in the microwave oven for the periods of 1, 2 and 3 minutes. The surface temperature of

the heated specimens was recorded using an infrared thermometer; these are depicted versus the different time intervals in Figure 4.8. Mixture variation does not seem to have a significant effect on temperature-heating time relationship. The temperature increased from 65°C to 116 °C within 2 minutes for both concretes.

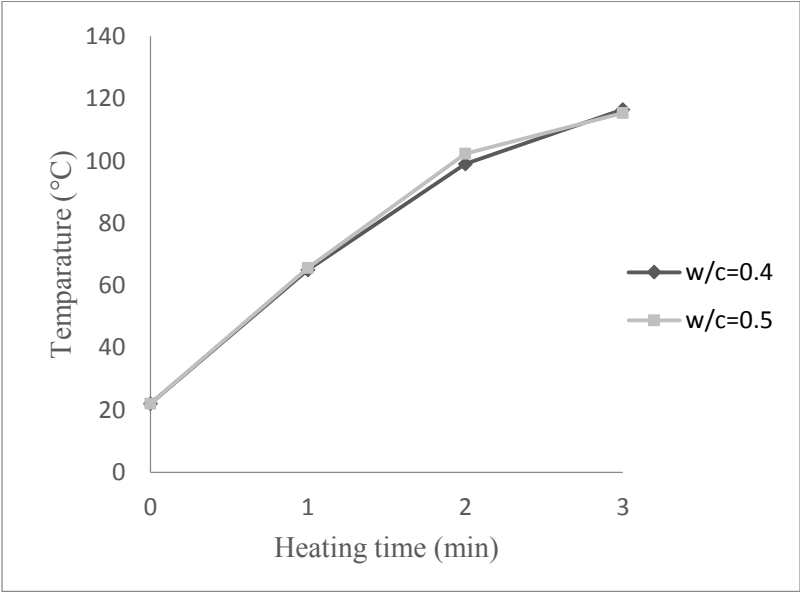


Figure 4.8 Temperature versus heating time

Sample mass was measured before and after microwave heating when they were cooled to the ambient temperature of the laboratory. Samples were then stored under water to become saturated before UPV measurements were made again. The average changes in the concrete weight and velocity due to the heating procedure were calculated and are shown in Figures 4.9 and 4.10 for w/c=0.4 and w/c=0.5, respectively.

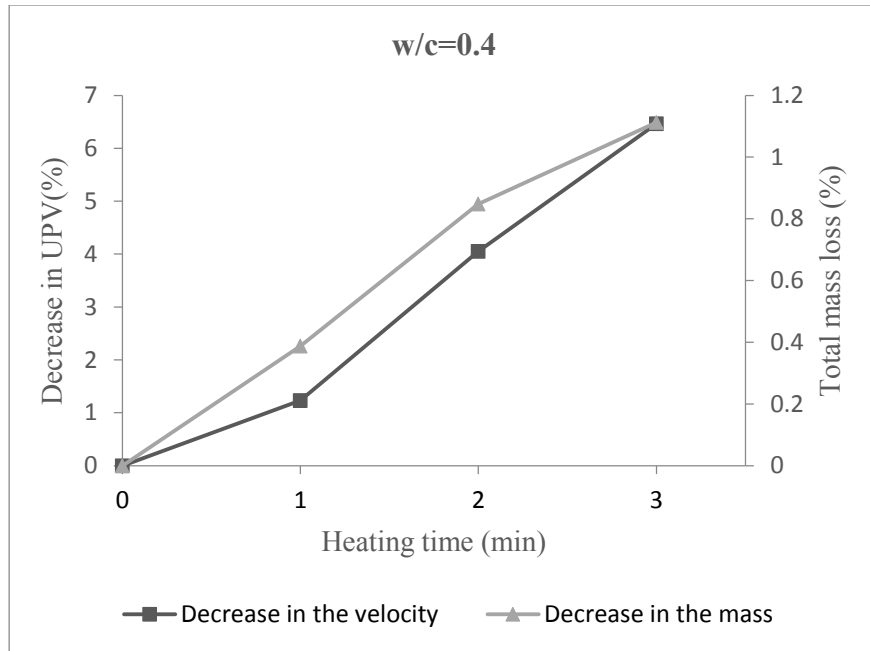


Figure 4.9 The effect of microwave heating on concrete mass and UPV for w/c=0.4

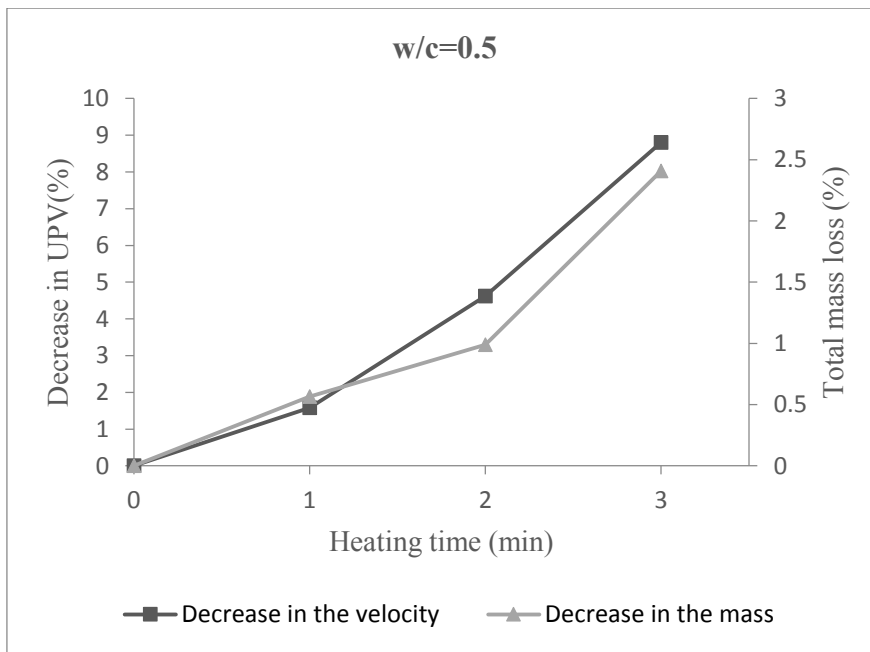


Figure 4.10 The effect of microwave heating on concrete mass and UPV for w/c=0.5

A gradual decrease in the mass and pulse velocity of concrete is evident as the heating time increases. This is an indication of severe microcrack propagation in the concrete due to thermal shock. Water is the main absorber of the irradiation energy induced by the microwave oven (Figg 1973). So, shrinkage cracking associated with the high rate of water evaporation from the pores of the rapidly dried specimen is responsible for the UPV reduction. Increasing the heating time from 1 to 3 minutes lowered the concrete velocity to 6.5% of its original value for $w/c=0.4$. For the other water-cement ratio concrete, a 9% decrease in the UPV could be observed corresponding to 2.4% mass loss which is more than twice the total loss in the mass of the concrete with $w/c=0.4$.

4.3.2 The effect of thermally-induced cracking on water absorption and electrical conductivity

The effect of rapid microwave drying on the rate of water absorption and electrical conductivity through concrete is presented in Figures 4.11 to 4.14. The individual results are also shown on the figures. An increase in concrete permeability with increasing the heating time is apparent. Generally, samples with lower water-cement ratio showed better performance in respect to drying shrinkage cracking. Since the higher water to cement ratio concrete is weaker in strength, it is more prone to damage induced by thermal stresses.

Data obtained for $w/c=0.4$, showed over 50% increase in the initial sorptivity of concrete after 3 minutes of rapid drying. The same period of microwave heating, caused more than 75% increase in the secondary sorptivity of these specimens. The condition is more severe in the higher water to cement ratio mixture in which samples heated for the period of 3 minutes absorbed more than 2 times as much water as control samples.

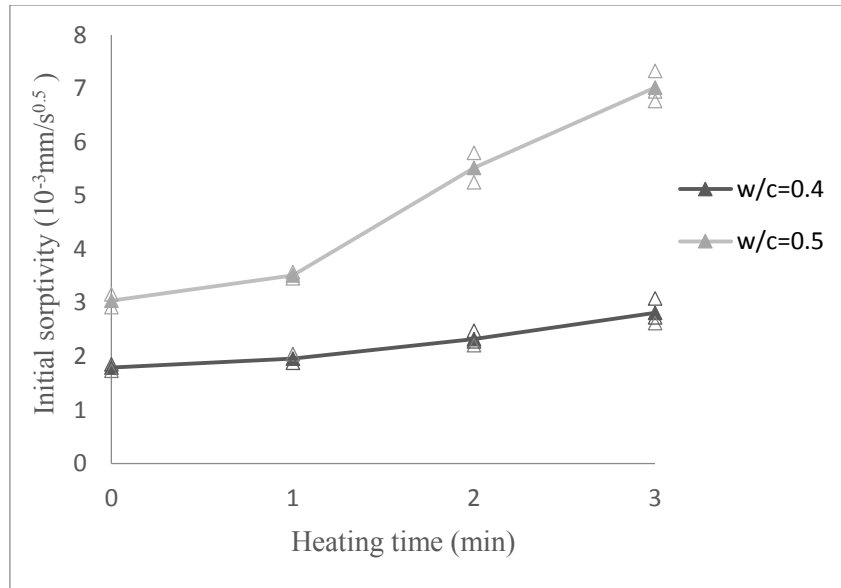


Figure 4.11 Relationship between initial sorptivity and heating time

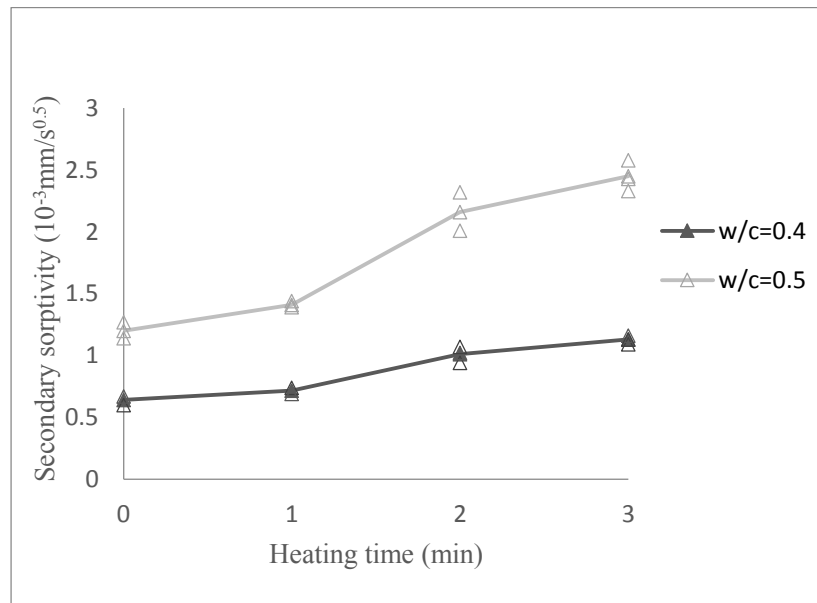


Figure 4.12 Relationship between secondary sorptivity and heating time

Rapid exposure to elevated temperature makes concrete less resistant against the electrical charges as well. Figure 4.14 shows the normalized electrical conductivity of the concrete as a function of the period samples were heated. The electrical conductivity of specimens with w/c=0.4 changed

by more than 36%, upon heating. Concrete with $w/c=0.5$ has experienced a higher rate of increase when the electrical conductivity increased from 12 mS/m at normal condition to 17.6 mS/m corresponding to 3 minutes microwave drying (45% growth).

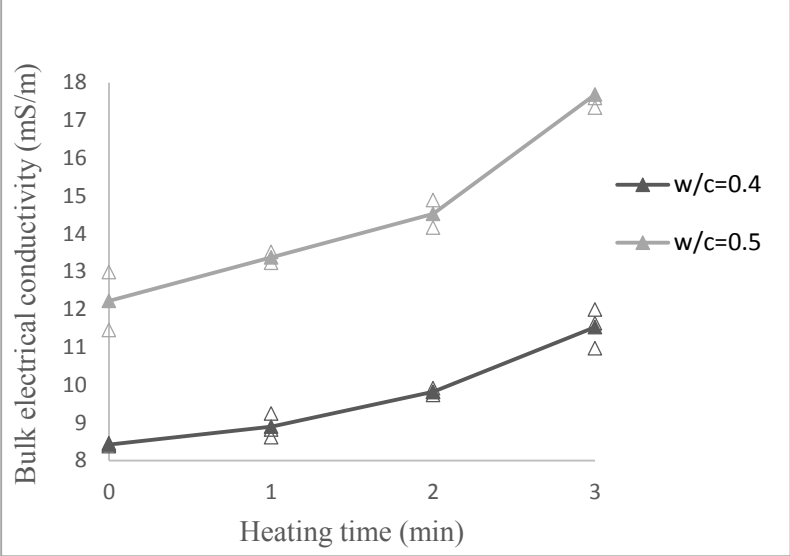


Figure 4.13 Relationship between bulk electrical conductivity and heating time

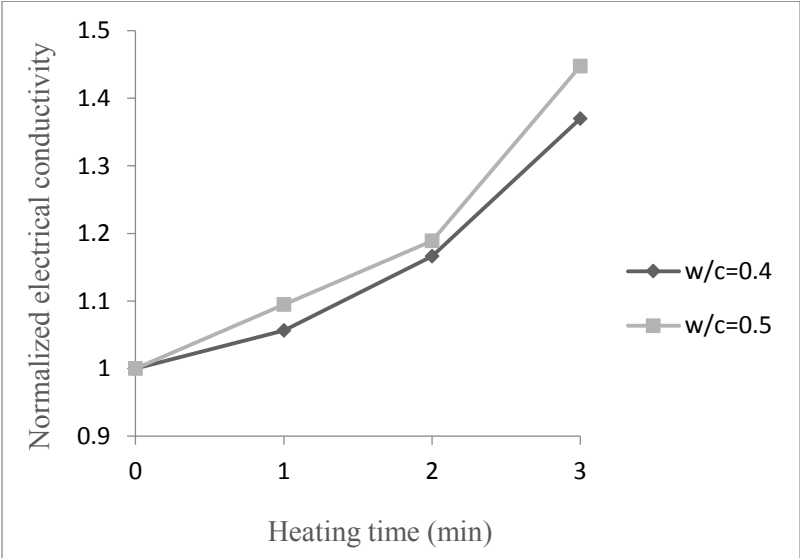


Figure 4.14 Relationship between normalized electrical conductivity and heating time

Thermal damage induced in concrete is due to the pressure induced by rapid water removal from the concrete which interconnects pores and internal flaws in concrete and generates a uniform network of microcracks. Tensile stresses derived from thermal mismatch between expansion coefficients of different concrete components is believed to be another factor leading to microcrack propagation in tangential, radial and axial directions around various particles. Therefore, drying shrinkage cracking has a direct impact on mass transport properties of concrete and resulting in higher permeability (Samaha and Hover 1992, Hearn 1999 and Choinska et al. 2007).

In contrast to the localized and discrete nature of microcracks induced under mechanical loading which do not have a significant influence on concrete permeability when tested upon unloading, drying shrinkage cracking are well distributed and linked throughout the concrete specimen which covers both mortar and aggregate-paste interface. Thus providing an easy access for water and aggressive substances through concrete and degrading its durability properties.

4.4 RESULTS FOR PHASE 3

4.4.1 The effect of consolidation degree on compressive strength of concrete

The relation between different levels of consolidation and the average compressive strength of concrete is shown in Table 4.3. The scatter among the compressive strength of unconsolidated samples was noticeably larger than the specimens normally compacted. This was leading to the coefficient of variation of 8% which is above the allowable limit indicated by ASTM C 39 for compressive strengths in the range of 17 to 32 MPa. Although the results of this study are outside of this range, the reason for the high coefficient of variation can be attributed to the high heterogeneity of non-vibrated concrete (Kaplan 1960).

The less porous nature of the lower water to cement ratio concrete makes it stronger regardless of the consolidation effect. In this experiment, compressive strength of fully consolidated concrete was reduced by 21% when the w/c ratio rose from 0.4 to 0.5.

As evident from the results, the compressive strength of unconsolidated samples significantly decreased compared with the fully vibrated concrete for both mixtures. The reduction in concrete strength for w/c=0.4 is 69% corresponding to the void content of 17.8%. A loss of approximately 25 MPa (67%) could be observed in the compressive strength of concrete containing 15.1% voids (w/c=0.5). The results are closely similar to the data obtained by Stewart (1951), Kaplan (1960) and Whiting et al. (1987) who found a 70% decrease in concrete strength by 15% decrease in degree of consolidation. The compressive strength of concrete is also reduced by over consolidation in both mixtures. But the effect of over vibration is much less pronounced than the influence of non-consolidation.

Table 4.3 Average compressive strength and the coefficient of variation for different consolidation levels

W/C ratio	Degree of consolidation	Average compressive strength (MPa)	Standard deviation (MPa)	Coefficient of variation (%) (Max=3.2%)
0.4	Full vibration	45.01	0.96	2.14
	Over-vibration	41.05	0.45	1.10
	Non-vibration	14.06	1.18	8.42
0.5	Full vibration	36.93	1.08	2.91
	Over-vibration	33.18	0.58	1.75
	Non-vibration	12.25	1.09	8.94

4.4.2 The effect of consolidation degree on ultrasonic pulse velocity

For each specimen, ultrasonic pulse velocity was measured at two perpendicular diametric directions. The average results of the UPV are plotted versus different consolidation conditions in Figure 4.15. The following abbreviations and symbols have been used in this section to make the figures more clear.

FM: Sample cut from the middle part of the fully consolidated concrete

NM: Sample cut from the middle part of the non-vibrated concrete

OT: Sample cut from the top end of the over consolidated concrete

OB: Sample cut from the bottom end of the over consolidated concrete

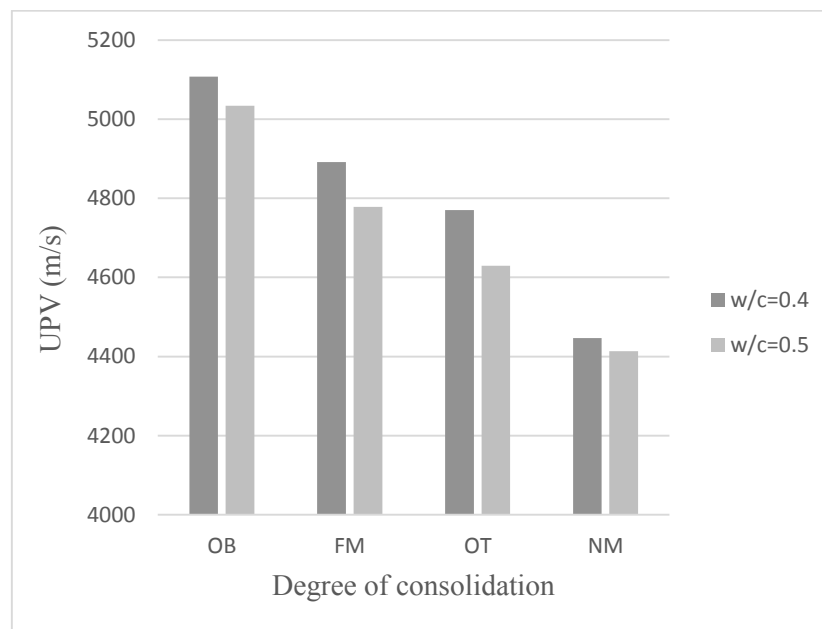


Figure 4.15 UPV versus degree of consolidation

As expected, concrete with the lower water-cement ratio has higher velocities at all consolidation levels. Incomplete consolidation (NM) results in a significant reduction in the pulse velocities of both mixtures. The reason is that the propagation of longitudinal pulse wave through concrete, as

an inhomogeneous material, will be scattered when encountering voids, cracks and internal heterogeneities. The non-uniform distribution of large interconnected air voids through the volume of the unconsolidated sample makes a delay in the pulse transmitting time by increasing the path length of the wave. The velocity of ultrasonic pulse will be decrease consequently.

The velocity of the non-vibrated specimens decreased by 9% and 7.6% compared with the velocity of fully vibrated concrete for $w/c=0.4$ and $w/c=0.5$, respectively. It appears that concrete with lower water-cement ratio is somehow more sensitive to the decrease in consolidation due to the larger amount of voids which were induced in lower slump mixture.

The changes in the UPV of the over-consolidated samples were also measured as a percentage of the fully vibrated concrete. There is an increase of 4.4% in the UPV of the samples cut from the bottom part of the over-vibrated concrete for $w/c=0.4$ compared to the fully consolidated samples. This value increased to 5.3% for $w/c=0.5$. On the other hand, samples cut from the top part of the cylinder have experienced a reduction of 2.5% and 3.1% in the UPV for $w/c=0.4$ and $w/c=0.5$, respectively. Similar observation was made by Popovics et al. (1990) (see Figure 2.25).

The reason is that ultrasonic pulse velocity through a medium will be influenced by the density and concentration of its components (Hearn 1999). Over consolidation results in the accumulation of bleed water and cement paste at the surface of the concrete and settlement of the coarse aggregates and solid particles at the bottom of the mold. Due to the more dense structure, bottom parts of the concrete subjected to segregation show much higher velocities than the top or middle sections. This influence is more apparent in the mixture with higher water-cement ratio and higher bleeding rate.

Simple comparison between the results of compressive strength and UPV, clearly indicates that the compressive strength is much more sensitive regarding to the degree of consolidation. For example, 17.8% void contents caused about 70% reduction in the compressive strength of concrete while the UPV was reduced by only 9% for the same amount of air voids.

4.4.3 The effect of consolidation degree on the water absorption test

Due to the presence of large air voids in the non-vibrated concrete samples, the contact area between the water and the surface of the specimen is not a full circular cross section. In these cases, the exposed surface area (a) which is used to measure the rate of water absorption in Equation 2.2 was measured using Auto CAD program (Figure 4.16). The average exposed surface area of the NM samples is approximately 7115 mm² compared with the fully vibrated samples with the average area equal to 8130 mm².

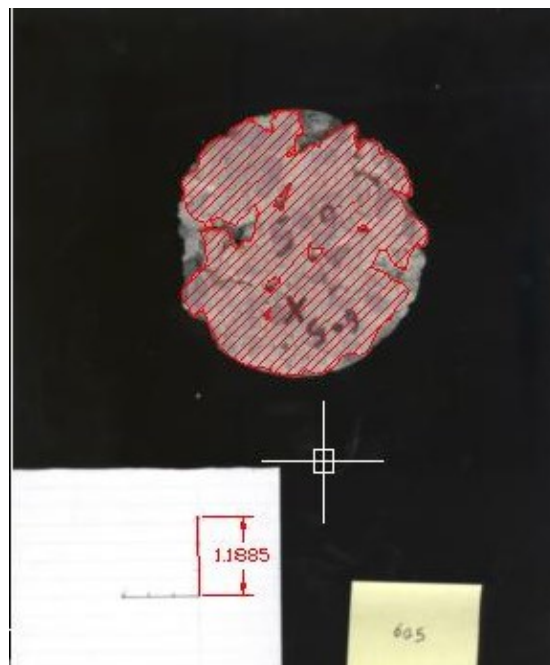


Figure 4.16 Measuring the exposed area of the NM sample by Auto CAD program

Figures 4.17 and 4.18 illustrate the results of initial and secondary sorptivity corresponding to different degrees of consolidation for both concrete mixtures. Non-vibrated samples with the correlation coefficient (R^2) below 0.9 were removed from the results. So the initial and secondary sorptivities were measured as the average of two specimens in these cases.

It is obvious that concrete with higher w/c ratio is more water permeable. For both mixtures tested, non-consolidation resulted in a significant increase in the initial and secondary sorptivities since the rate of water absorption through concrete is directly affected by the pore volume and connectivity of the capillaries (Samaha and Hover 1992). A 15.1% void content induced in concrete with w/c=0.5, causes an increase in the initial sorptivity up to 6 times of the value obtained for fully consolidated samples. The mixture with the lower w/c ratio was even more severely degraded where the sorptivity of concrete having 17.8% voids jumped from 0.00169 to 0.0117 $\text{mm/s}^{0.5}$ (7 times increase).

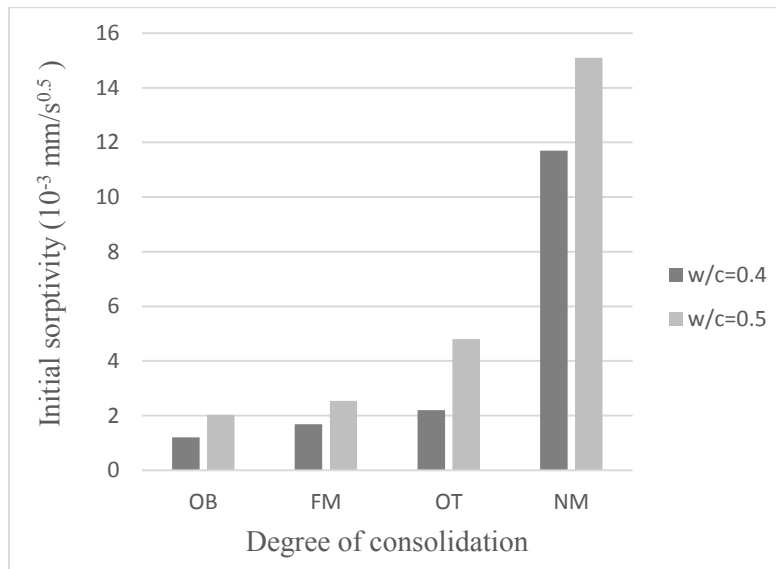


Figure 4.17 Initial sorptivity versus consolidation degree

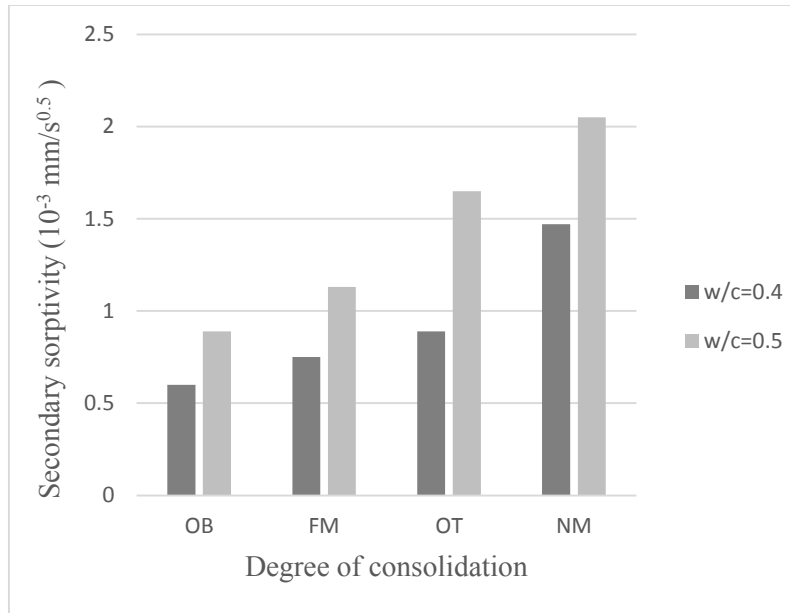


Figure 4.18 Secondary sorptivity versus consolidation degree

Comparing the data of Figures 4.17 and 4.18 would imply the fact that the presence of air voids has much less effect on the secondary absorption than initial absorption. Since the major amount of water was absorbed by the rapid initial suction during the first hours of exposure, further rate of water ingress through concrete is lowered. The maximum increase in the secondary sorptivity of non-vibrated samples is slightly below 100% which is occurred in the w/c=0.4.

Drying shrinkage cracking observed accompanied by the evaporation of bleed water from the concrete surface enables the higher rate of short term and long term absorption in OT specimens. An increase of 30% and 80% in the initial sorptivity of these samples could be observed for w/c=0.4 and 0.5, respectively. However, over consolidation at the bottom parts somehow improved the concrete permeability against water ingress due to the lower absorptivity of the aggregates and expulsion of the entrapped air during excessive period of vibration.

The damage induced by saw cutting was assumed to be equal for the fully vibrated, non- vibrated and over-vibrated samples. Therefore, the effect of cutting was ignored from these results.

4.4.4 The effect of consolidation degree on bulk electrical conductivity and bulk electrical resistivity

The results of concrete electrical conductivity are plotted in Figure 4.19. Both concrete mixtures are similarly affected by the degree of consolidation. It was not possible to measure the electrical conductivity of non-consolidated (NM) samples due to the large interconnected voids. Concrete conductivity greatly depends on the volume, size and connectivity of the pores. Samples sliced from the top part of the over consolidated concrete exhibit the highest conductivity in both water-cement ratios. This is most likely due to the presence of bleed water and increased fine particles at the top section which impairs the quality of the near surface zone. On the other hand, aggregate segregation in OB specimens decreased the electrical conductivity of concrete by as much as 50% for $w/c=0.5$ and 27% for $w/c=0.4$ with respect to the normally vibrated concrete.

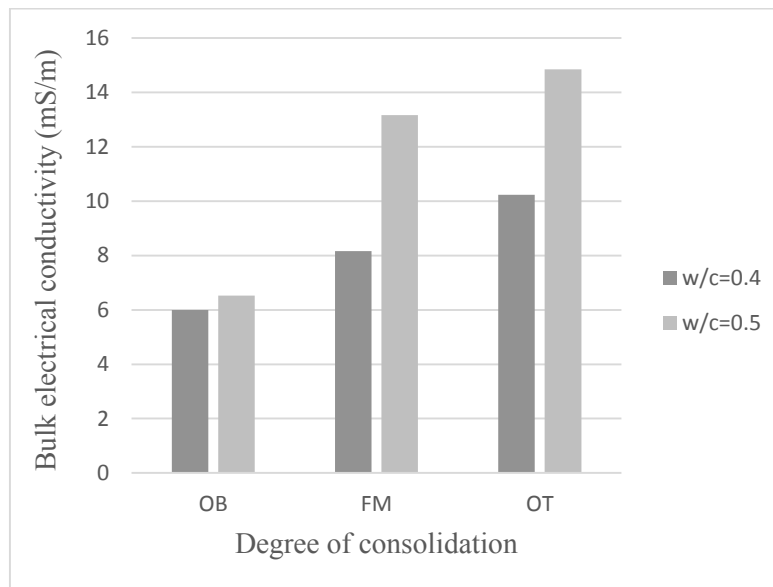


Figure 4.19 Relationship between consolidation degree and electrical conductivity

Since the electrical conductivity of unconsolidated samples could not be measured, all samples in phase 3 were tested for the bulk electrical resistivity which is the inverse of electrical conductivity.

Figure 4.20 presents the results for $w/c=0.4$ and $w/c=0.5$. Here again, there is a decrease in resistivity of higher water-cement ratio concrete which indicates a more permeable microstructure.

OB specimens behave in a same way to electrical resistivity as they did with the conductivity versus consolidation level. For $w/c=0.5$, the electrical resistivity will be doubled when over vibrated in the bottom of the cylinder. Also, concrete with $w/c=0.4$ are 80% more resistive than the fully vibrated samples.

Generally, the higher amounts of electrical resistivity reflect more durable concrete. But unlike expected, the values of electrical resistivity for non-vibrated samples are essentially higher than other specimens in both concrete mixtures. This may be explained by the presence of the large, irregular and interconnected air voids in the concrete volume which will increase the path length and tortuosity for the electrical current to pass through the specimen (refer to the Figure 3.2). Thus, the longer path length exists in the highly porous unconsolidated specimens leads to an erroneous increase in its electrical resistivity.

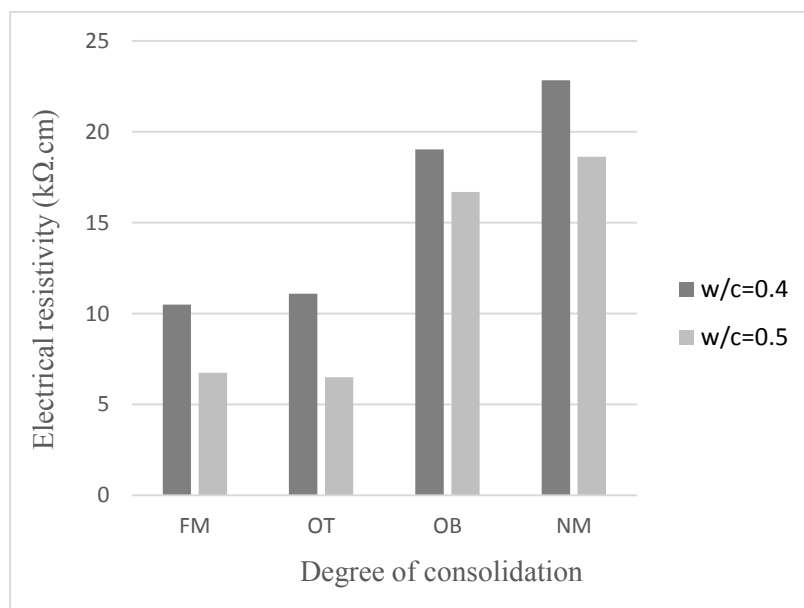


Figure 4.20 The effect of consolidation on electrical resistivity

5 CONCLUSIONS AND RECOMMENDATIONS

5.1 CONCLUSIONS

This project was aimed at evaluating the influence of construction defects on the results of two common standardized durability tests. Concrete samples were cracked to various extents either by mechanical loading or thermal loading. Moreover, some specimens were subjected to different levels of consolidation to reflect the occurrence of poor field construction practices. Mass transport properties of concrete were assessed based on the standard test methods including water absorption, electrical conductivity and ultrasonic pulse velocity.

The safety factors considered in the design codes, limit the concrete service loads to 65% of its capacity. The results of this research indicate that concrete durability will not be endangered by microcrack development under such stress levels. However, if concrete is located in an environmental condition subjected to high rate of evaporation and high thermal gradients; cracking is a serious durability concern since the propagation of shrinkage cracking under rapid heating was found to be far more deleterious than the effect of load induced microcracks even at high stress levels. Therefore, special precaution is required to protect concrete by using shrinkage resistant mixtures, proper curing procedures or using aggregates of low thermal expansion coefficients. In addition, the results of this study regarding the effect of consolidation degree on concrete durability can be used to develop quality control specifications.

The specific conclusions drawn from the results of this study can be summarized as follows:

1. The propagation of interconnected mortar cracking near failure seems to be the governing factor increasing the rate of water absorption and electrical conductivity of concrete, while bond cracking formed at low stress levels is less influential.

2. The amount of water absorption did not show a significant response to increasing the stress level up to approximately $0.8f_u$. This was followed by the maximum increase of 40% in the secondary sorptivity of $w/c=0.4$ at 90% of the ultimate capacity.
3. Similarly, the measured electrical conductivity test was insensitive to the stress/strength ratio below $0.7f_u$. However, beyond that point concrete becomes less resistant by more than 20% and 30% for $w/c=0.5$ and 0.4 , respectively.
4. Observations based on the ultrasonic pulse velocity support the results obtained by sorptivity and electrical conductivity tests indicating that concrete is unaffected by tensile induced cracking below 70% of the peak strength due to the microcrack recovery after unloading.
5. Although the values of water absorption and electrical conductivity are higher for $w/c=0.5$, samples with lower water to cement ratio are more sensitive to the degree of load induced damage.
6. A well-distributed network of interconnected cracking induced by harsh microwave heating has far more deleterious effect on water absorption and electrical conductivity of concrete compared with the formation of single, non-distributed crack pattern under short term tensile loading.
7. The water sorptivity and electrical conductivity of concrete followed an increasing trend with increasing the heating time. A gradual decrease in the UPV and concrete mass was also observed as the microwave heating duration increased.

8. Increasing the rapid drying time from 1 to 3 minutes caused more than two times increase in water sorptivity and 45% increase in the electrical conductivity of concrete with $w/c=0.5$.
9. In general, damage resulting from thermal loading is more pronounced in higher water to cement ratio concrete due to its higher porosity and lower strength.
10. The presence of air voids in the non-vibrated samples makes them about 70% weaker in compressive strength corresponding to 9% decrease in the UPV.
11. The initial water sorptivity of unconsolidated samples is 7 times larger than that of fully vibrated concrete. This is a dramatic difference compared with the damage results from both loading and thermal cracking.
12. Over consolidation also changes the transport properties of concrete. The higher density of the concrete at the bottom parts of the cylinder in addition to the air expulsion under excessive vibration, slightly improves the concrete resistance against water and electrical conduction. In contrast, the upward movement of water and fine particles increased the capillary porosity of the top surface area.
13. While interpreting the results of electrical resistivity for non-vibrated samples, the relevant formulas must be modified in order to compensate for the effect of length increment occurred by the presence of large interconnected voids. Otherwise, resistivity test provides misleading evaluation of concrete durability.

5.2 RECOMMENDATIONS

1. It was concluded that the durability of concrete will not be endangered by microcrack propagation below 70% of the peak tensile strength. However, concrete response to the cyclic or sustained loading cannot be predicted based on the results of this study.
2. In order to eliminate the influence of microcrack recovery upon unloading, more attempts must be made to find a way for measuring the water absorption and chloride permeability of concrete samples while being loaded.
3. To better understand the effect of mixture variation on durability properties of concrete, it is suggested to consider the wider ranges of water to cement ratios. The effect of aggregate size and supplementary cementing materials on these results is also of interest for future work.
4. Ultrasonic pulse velocity is a useful method to detect the presence of flaws and microcracks in concrete. But microscopic examination such as scanning electron microscopy (SEM) or CT scan is desirable in order to determine crack characteristics such as width, length and connectivity.
5. Since the application of electrical conductivity and electrical resistivity tests was not possible to evaluate the permeability of non-vibrated specimens, other performance test methods such as freezing and thawing and chloride bulk diffusion test could be conducted as an extension to this study.

6 REFERENCES

ACI 309R-05. (2005). “Guide for Consolidation of Concrete”. *American Concrete Institute*, Farmington Hills, Michigan.

ACI 309.2R-98. (2005). “Identification and Control of Visible Effects of Consolidation on Formed Concrete Surfaces”. *American Concrete Institute*, Farmington Hills, Michigan.

ASTM Standard C39. (2005). “Standard Test Method for Compressive Strength of Cylindrical Concrete Specimens”. *ASTM International*, West Conshohocken, PA, 2005, DOI: 10.1520/C0039-05, www.astm.org.

ASTM Standard C138. (2010). “Standard Test Method for Density (Unit Weight), Yield, and Air Content (Gravimetric) of Concrete”. *ASTM International*, West Conshohocken, PA, 2005, DOI: 10.1520/C0138-10, www.astm.org.

ASTM Standard C143. (2000). “Standard Test Method for Slump of Hydraulic-Cement Concrete”. *ASTM International*, West Conshohocken, PA, 2005, DOI: 10.1520/C0143-00, www.astm.org.

ASTM Standard C192. (2007). “Standard Test Method for Making and Curing Concrete Test Specimens in the Laboratory”. *ASTM International*, West Conshohocken, PA, 2007, DOI: 10.1520/C0192-07, www.astm.org.

ASTM Standard C231 (2010). “Standard Test Method for Air content of Freshly Mixed Concrete by the Pressure Method”. *ASTM International*, West Conshohocken, PA, 2005, DOI: 10.1520/C0231-10, www.astm.org.

ASTM Standard C232. (2009). “Standard Test Methods for Bleeding of Concrete”. *ASTM International*, West Conshohocken, PA, 2009, DOI: 10.1520/C0232-09, www.astm.org.

ASTM Standard C496. (2011). “Standard Test Method for Splitting Tensile Strength of Cylindrical Concrete Specimens”. *ASTM International*, West Conshohocken, PA, 2011, DOI: 10.1520/C496-11, www.astm.org.

ASTM Standard C597. (2009). “Standard Test Method for Pulse Velocity Through Concrete”. *ASTM International*, West Conshohocken, PA, 2009, DOI: 10.1520/C0597-09, www.astm.org.

ASTM Standard C1202. (2005). “Standard Test Method for Electrical Indication of Concrete’s Ability to Resist Chloride Ion Penetration”. *ASTM International*, West Conshohocken, PA, 2005, DOI: 10.1520/C1202-05, www.astm.org.

ASTM Standard C1585. (2004). “Standard Test Method for Measurement of Rate of Absorption of Water by Hydraulic-Cement Concretes”. *ASTM International*, West Conshohocken, PA, 2004, DOI: 10.1520/C1585-04, www.astm.org.

ASTM Standard C1760. (2012). “Standard Test Method for Bulk Electrical Conductivity of Hardened Concrete”. *ASTM International*, West Conshohocken, PA, 2012, DOI: 10.1520/C1760-12, www.astm.org.

Acciani, G., Fornarelli, G., Giaquinto, A., & Maiullari, D. (2010). Nondestructive evaluation of defects in concrete structures based on finite element simulations of ultrasonic wave propagation. *Nondestructive Testing and Evaluation*, 25(4), 289-315.

- Aldea, C. M., Ghandehari, M., Shah, S. P., & Karr, A. (2000). Estimation of water flow through cracked concrete under load. *ACI Materials Journal*, 97(5), 567-575.
- Aldea, C. M., Shah, S. P., & Karr, A. (1999). Effect of cracking on water and chloride permeability of concrete. *Journal of Materials in Civil Engineering*, 11(3), 181-187.
- Al-Khaja, W. A. (1997). Influence of temperature, cement type and level of concrete consolidation on chloride ingress in conventional and high-strength concretes. *Construction and Building Materials*, 11(1), 9-13.
- Banthia, N., Biparva, A., & Mindess, S. (2005). Permeability of concrete under stress. *Cement and Concrete Research*, 35(9), 1651-1655.
- Basheer, L., Kropp, J., & Cleland, D. J. (2001). Assessment of the durability of concrete from its permeation properties: a review. *Construction and Building Materials*, 15(2), 93-103.
- Bhargava, A., & Banthia, N. (2006). Measurement of concrete permeability under stress. *Experimental Techniques*, 30(5), 28-31.
- Carrasquilio, R. L., & Nilson, A. H. (1981). Microcracking and behavior of high strength concrete subject to short-term loading. *ACI Journal Proceedings*, 78(3), 179-186.
- Castro, J., Bentz, D., & Weiss, J. (2011). Effect of sample conditioning on the water absorption of concrete. *Cement and Concrete Composites*, 33(8), 805-813.
- Choinska, M., Khelidj, A., Chatzigeorgiou, G., & Pijaudier-Cabot, G. (2007). Effects and interactions of temperature and stress-level related damage on permeability of concrete. *Cement and Concrete Research*, 37(1), 79-88.

Collepari, M., Marcialis, A., & Turriziani, R. (1972). Penetration of chloride ions into cement pastes and concretes. *Journal of the American Ceramic Society*, 55(10), 534-535.

Figg, J. (1974). Microwave heating in concrete analysis. *Journal of Applied Chemistry and Biotechnology*, 24(3), 143-155.

Fu, Y. F., Wong, Y. L., Poon, C. S., Tang, C. A., & Lin, P. (2004). Experimental study of micro/macro crack development and stress–strain relations of cement-based composite materials at elevated temperatures. *Cement and Concrete Research*, 34(5), 789-797.

Gerard, B., Breysse, D., Ammouche, A., Houdusse, O., and Didry, O. (1996). Cracking and permeability of concrete under tension. *Materials and Structures*, 29(3), 141-151.

Hall, C., & Raymond Yau, M. H. (1987). Water movement in porous building materials—IX. The water absorption and sorptivity of concretes. *Building and Environment*, 22(1), 77-82.

Hearn, N. (1999). Effect of shrinkage and load-induced cracking on water permeability of concrete. *ACI Materials Journal*, 96(2), 234-241.

Hoseini, M., Bindiganavile, V., & Banthia, N. (2009). The effect of mechanical stress on permeability of concrete: a review. *Cement and Concrete Composites*, 31(4), 213-220.

Huang, Q. (2006). *Influences of Cracks on Chloride-induced Corrosion in Reinforced Concrete Structures*. M.A.Sc. thesis, Chalmers University of Technology, Gothenburg, Sweden. 81 pages.

Jones, R. (1952). A method of studying the formation of cracks in a material subjected to stress. *British Journal of Applied Physics*, 3(7), 229-232.

Josserand, L., Coussy, O., & de Larrard, F. (2006). Bleeding of concrete as an ageing consolidation process. *Cement and Concrete Research*, 36(9), 1603-1608.

Kaplan, M. F. (1960). Effects of Incomplete Consolidation on Compressive and Flexural Strength, Ultrasonic Pulse Velocity, and Dynamic Modulus of Elasticity of Concrete. In *ACI Journal Proceedings*. 56(3), 853-868.

Kelly, J. W. (1981). Cracks in Concrete. *Concrete Construction*, 26(9).

Kermani, A. (1991). Permeability of stressed concrete: Steady-state method of measuring permeability of hardened concrete studies in relation to the change in structure of concrete under various short-term stress levels. *Building Research and Information*, 19(6), 360-366.

Knab, L. I., Blessing, G. V., & Clifton, J. R. (1983). Laboratory evaluation of ultrasonic for crack detection in concrete. *ACI Journal Proceedings*, 80(1), 17-27.

Kosmatka, S. H., & Panarese, W. C. (2002). *Design and control of concrete mixtures*. (7th edition). Cement Association of Canada. Ottawa, Canada. 368 pages.

Krishnaswamy, K. T. (1969). Microcracking of plain concrete under uniaxial compressive loading. *Indian Concrete Journal*, 43(4), 143-145.

Kristensen, L., & Hansen, T. C. (1994). Cracks in concrete core due to fire or thermal heating shock. *ACI Materials Journal*, 91(5), 453-459.

Kumar Mehta, P. (2000). Durability-critical issues for the future. *CANMET/ACI. Séminaire international*. Les ciments et bétons à haut volume de cendres volantes : leur rôle dans le développement durable : (Lyon, 29 novembre 2000) CANMET / ACI. Séminaire international, Lyon, France.

- Lim, C. C., Gowripalan, N., & Sirivivatnanon, V. (2000). Microcracking and chloride permeability of concrete under uniaxial compression. *Cement and Concrete Composites*, 22(5), 353-360.
- Lin, Z., & Wood, L. (2003). Concrete uniaxial tensile strength and cylinder splitting test. *Journal of Structural Engineering*, 129(5), 692-698.
- Loo, Y. H. (1992). A new method for microcrack evaluation in concrete under compression. *Materials and Structures*, 25(10), 573-578.
- Ludirdja, D., Berger, R. L., & Young, J. (1989). Simple method for measuring water permeability of concrete. *ACI Materials Journal*, 86(5), 433-439.
- Mahmood, A. (2008). Structural Health Monitoring Using non Destructive Testing of Concrete. Bachelor thesis, National Institute of Technology Rourkela. India.
- Malhotra, V. M., & Carino, N. J. (Eds.). (2004). *Handbook on non-destructive testing of concrete*. CRC press, Pennsylvania, United States.
- Martys, N. S., & Ferraris, C. F. (1997). Capillary transport in mortars and concrete. *Cement and Concrete Research*, 27(5), 747-760.
- Mehta, P. K., & Burrows, R. W. (2001). Building durable structures in the 21st century. *Concrete International*, 23(3), 57-63.
- Mehta, P. K., & Monteiro, P. J. (2006). *Concrete: microstructure, properties, and materials* (3rd Edition). New York: McGraw-Hill.
- Menzel, C. A. (1954). Causes and prevention of crack development in plastic concrete. *Proceedings of the Portland Cement Association*, 130, 136.

Meyers, B. L. (1969). Relationship between time-dependent deformation and microcracking of plain concrete. *ACI Journal Proceedings*, 66(1), 60-68.

Philleo, R. (1958). Some physical properties of concrete at high temperatures. *ACI Journal Proceedings*, 54(4), 857-864.

Popovics, S., Rose, J. L., & Popovics, J. S. (1990). The behaviour of ultrasonic pulses in concrete. *Cement and Concrete Research*, 20(2), 259-270.

Raju, N. K. (1970). Small concrete specimens under repeated compressive loads by pulse velocity technique. *Journal of Materials*, 5(2), 262-272.

Ramamoorthy, S. K., Kane, Y., & Turner, J. A. (2004). Ultrasound diffusion for crack depth determination in concrete. *The Journal of the Acoustical Society of America*, 115(2), 523-529.

Rasheeduzzafar, A. S. (1989). Influence of construction practices on concrete durability. *ACI Materials Journal*, 86(6), 566-575.

Saito, M., & Ishimori, H. (1995). Chloride permeability of concrete under static and repeated compressive loading. *Cement and Concrete Research*, 25(4), 803-808.

Samaha, H. R., & Hover, K. C. (1992). Influence of microcracking on the mass transport properties of concrete. *ACI Materials Journal*, 89(4), 416-424.

Santiago, S. D., & Hilsdorf, H. K. (1973). Fracture mechanisms of concrete under compressive loads. *Cement and Concrete Research*, 3(4), 363-388.

Shah, A. A., & Ribakov, Y. (2012). Damage detection in concrete using nonlinear signal attenuation ultrasound. *Latin American Journal of Solids & Structures*, 9(6), 713-730.

- Shah, S. P., & Chandra, S. (1970). Fracture of concrete subjected to cyclic and sustained loading. *ACI Journal Proceedings*, 67(10), 816-827.
- Shahroodi, A. (2010). *Development of Test Methods for Assessment of Concrete Durability for Use in Performance-Based Specifications*. M.A.Sc. thesis, University of Toronto, Toronto, Canada. 260 pages.
- Shokouhi, P., and Niederleithinger, E. (2012). Damage characterization in concrete using diffuse ultrasound. *In Review of Proceeding in Quantitative Non-destructive Evaluation*, Burlington, VT, 17-22 July 2011. 1430(1). 1477-1484.
- Shokouhi, P., Wöstmann, J., Schneider, G., Milmann, B., Taffe, A., & Wiggerhauser, H. (2011). Nondestructive Detection of Delamination in Concrete Slabs. *Transportation Research Record: Journal of the Transportation Research Board*, 2251(1), 103-113.
- Sillanpaa, M. (2010). *The effect of cracking on chloride diffusion in concrete*. M.A.Sc. thesis, Aalto University. Espoo, Finland. 134 pages.
- Singh, B. (2013). Bleeding in concrete. *International Journal of Civil Engineering and Technology*. 4(2), 247-249
- Spragg, R., Bu, Y., Snyder, K., Bentz, D., & Weiss, J. (2013). Electrical testing of cement-based materials: role of testing techniques, sample conditioning, and accelerated curing. *Joint Transportation Research Program*, Indiana department of transportation and Purdue University.
- Stanish, K. D., Hooton, R. D., & Thomas, M. D. A. (1997). Testing the chloride penetration resistance of concrete: a literature review. *FHWA contract DTFH61*, 19-22.

Stewart, D. A. (1951). The design and placing of high quality concrete. *E. & F. N. Spon*. London, England.

Sugiyama, T.; Bremner, T. W.; and Holm, T. A., (1993). Effect of Stress on Chloride Permeability in Concrete. *Durability of Building Materials and Components*, 6(1), 239-248.

PROCEQ, (2012). Resipod operating instructions, SA, Schwerzenbach.

Topçu, İ. B., & Elgün, V. B. (2004). Influence of concrete properties on bleeding and evaporation. *Cement and Concrete Research*, 34(2), 275-281.

Wainwright, P. J., & Ait-Aider, H. (1995). The influence of cement source and slag additions on the bleeding of concrete. *Cement and Concrete Research*, 25(7), 1445-1456.

Wang, K., Jansen, D. C., Shah, S. P., & Karr, A. F. (1997). Permeability study of cracked concrete. *Cement and Concrete Research*, 27(3), 381-393.

Whiting, D., G. W. Seegebrecht, and S. Tayabji. (1987). Effect of degree of consolidation on some important properties of concrete. *ACI Special Publication*, 96. 125-160.

Wiens, U., Meng, B., Schroeder, P., and Schiessl, P., (1997) Microcracking in high performance concrete from model to the effect on concrete properties, self-desiccation and its importance on concrete technology, Ed. B. Persson, G. Fagerlund, Lund, Sweden, 193-208.

Wu, T. T., & Lin, T. F. (1998). The stress effect on the ultrasonic velocity variations of concrete under repeated loading. *ACI Materials Journal*, 95(5), 519-524.

Wu, C.H., & Wang, J.Y. (2000). The behavior of ultrasonic waves propagating in concrete using the ultrasonic-pulse methods to measure the depths of cracks in concrete. *Proceedings of the*

International Symposium on Automation and Robotics in Construction and Mining 17, 1-6.

Retrieved from http://www.iaarc.org/publications/fulltext/isarc2000-204_MA3.pdf

Yang, Z. (2004). *Assessing cumulative damage in concrete and quantifying its influence on life cycle performance modeling*. PhD thesis, Purdue University, West Lafayette, Indiana. 245 pages.

Yang, Z., Weiss, W. J., & Olek, J. (2006). Water transport in concrete damaged by tensile loading and freeze–thaw cycling. *Journal of Materials in Civil Engineering*, 18(3), 424-434.

Yim, H. J., Kim, J. H., Kwak, H. G., & Kim, J. K. (2013). Evaluation of internal bleeding in concrete using a self-weight bleeding test. *Cement and Concrete Research*, 53, 18-24.

Yoon, I. S., Schlangen, E., Rooij, M. R. D., & Van Breugel, K. (2007). The effect of cracks on chloride penetration into concrete. *Key Engineering Materials*, 348, 769-772.